FAST MEMORY EFFICIENT EVALUATION OF SPHERICAL POLYNOMIALS AT SCATTERED POINTS

KAMEN IVANOV AND PENCHO PETRUSHEV

ABSTRACT. A method for fast evaluation of spherical polynomials (band-limited functions) at many scattered points on the unit 2-d sphere is presented. The method relies on the sub-exponential localization of the father needlet kernels and their compatibility with spherical harmonics. It is fast, local, memory efficient, numerically stable and with guaranteed (prescribed) accuracy. The speed is independent of the band limit and depends logarithmically on the precision. The method can be also applied for approximation on the sphere, verification of spherical polynomials and for fast generation of surfaces in computer-aided geometric design. It naturally generalizes to higher dimensions.

1. INTRODUCTION

In this paper we take on the problem for effective computation of the values of high degree (> 2000) 2-d spherical polynomials at scattered points on the sphere. We seek an algorithm which is accurate, fast, stable and memory efficient. This problem is important for many areas, where high degree spherical harmonics are employed. A targeted application and motivation for this undertaking is the problem for fast efficient computation of the values of the geoid undulation determined from the Earth Gravitational Model EGM2008 of NGA [14].

The problem for fast evaluation of a *spherical* polynomial at many scattered points on the unit sphere $\mathbb{S}^2$ in $\mathbb{R}^3$ is usually divided into two subproblems:

- **(i):** Evaluate a spherical polynomial of degree N given by its coefficients at *regular grid points* on $\mathbb{S}^2$;
- **(ii):** Evaluate at J *scattered points* a spherical polynomial of degree N given by its values at regular grid points.

"Regular grid points on $\mathbb{S}^2$" may have several different meanings. As is well known there are no equally spaced points on the sphere, except for the vertices of the five Platonic solids. Hence, asymptotically equally distributed points may be considered as regular grid points. On the other hand the regular grid points may be defined as points which are equally spaced with respect to their *spherical* coordinates (θ, λ). We shall adopt the latter notion. It has the obvious drawback that the grid points congregate near the poles, but this is fully compensated by the possibility of applying fast Fourier methods. The mesh size in each coordinate is $O(N^{-1})$, thus having a total of $O(N^2)$ points the grid is compatible with $(N+1)^2$, the number of polynomial coefficients (see §2.1).

A direct evaluation of a spherical polynomial of degree N at $O(N^2)$ grid points has computational complexity $O(N^4)$. Using straightforward separation of variables and the associated Legendre functions recurrence formulas the complexity of problem (i) is reduced to $O(N^3)$ and the algorithm is numerically stable.

The first two-dimensional fast Fourier method on the sphere (for expansion, not evaluation) was developed by Driscoll and Healy [2]. Mohlenkamp presented in [9] two algorithms for *approximate* solution of problem (i) with costs $O(N^{5/2} \log N)$ and $O(N^2(\log N)^2)$. The stability of the original algorithms in [2, 9] was problematic and subsequent efforts were made for their stabilization. Another approach for approximate solution of (i) with $O(N^2 \log N)$ operations was recently proposed by Tygert [16]. It is based on the multi-pole method; the algorithm is claimed to be stable.

A standard method for solving problem (ii) is by using bivariate spline interpolation, see e.g. [8]. In principle this method experiences accuracy problems because the sets of spherical splines and polynomials have small intersection. Consequently, the error of approximation is $O((hN)^r)$, where h is the mesh size, N is the degree of the polynomial being approximated and r is the order of the spline interpolant (the constant depends on the uniform norm of the polynomial). The accuracy can be improved by decreasing the mesh size h in (i) or by restricting the set of spherical polynomials to those which approximate functions with prescribed smoothness. The decrease of the mesh size causes both memory and speed problems. Restrictions on the spherical polynomial set narrows the range of problem (ii) and lead to undesirable high value of N in the case of low smoothness of the approximated function.

In this paper we present an alternative method for solving problem (ii), based on the spherical "needlets" introduced in [11, 12]. We propose a new approximation scheme based on "father needlets". These are kernels on the sphere which reproduce high order spherical harmonics and are sub-exponentially localized and hence are perfectly well suited for approximation in the uniform norm.

The method requires problem (i) to be solved in advance on a regular grid consisting of $O(N^2)$ points. The father needlets being spherical harmonics friendly allow to achieve the desired accuracy ε using a grid with larger mesh size than when using e.g. spline interpolation. This distinctive feature of our method leads to modest requirements on the computer memory size, and hence makes it attractive for *compressed* (memory efficient) evaluation of spherical polynomials. Furthermore, the grid depends only on the polynomial degree N and is independent of the polynomial coefficients and the targeted accuracy. Thus better accuracy can be achieved without solving problem (i) for a new refined grid.

The method is *fast* because it is *local* in the sense that only the polynomial values from a small neighborhood of the point of computation are used. More precisely, we determine within an arbitrary precision ε the value of a polynomial at a given point using its values at $\nu_\varepsilon = O((\log(1/\varepsilon))^2 (\log\log(1/\varepsilon))^{2+2\beta})$ neighboring grid points, where $\beta > 0$ (say $\beta = 1/2$). Thus the number of operations for solving (ii) is $O(\nu_\varepsilon J)$. As the form of ν_ε indicates, the precision increase is achieved by a slight enlargement of the point neighborhood. On the other hand the number of floating-point operations does not depend on the polynomial degree. Let us also point out that the method is *numerically stable*.

The method has been implemented in MATLAB 7.2 with double-precision variables. Variable precision arithmetic is *not needed* for achieving accuracy 10^{-10} in evaluating spherical polynomials of degree several thousand. All our experiments were performed in real time on a standard 1.6 GHz PC with 1 GB of RAM. The method has been intensively tested for degrees between 500 and 2160 (see §5). These tests (and other experiments with polynomials of degree up to 8000) confirm the features of our method outlined above.

The paper is organized as follows. The formulation of the problem and the theoretical basis for its solution by our method is given in §2. In §3 we discuss all parts of the method, describe the relations between the parameters and present the method in an algorithmic form. In §4 we generalize our method to dimensions $d > 2$ and present some of its applications to other problems. Some numerical experiments are described in §5. Section 6 contains our concluding remarks.

We will denote by c positive constants which may vary at every appearance and by $\bar{c}, \tilde{c}, c', c''$ and the alike positive constants which preserve their values throughout the paper. The relation $f \sim g$ means $cf \leq g \leq cf$, while $f \approx g$ is used when $f/g \to 1$ under an appropriate limit of the argument.

2. Theoretical underpinning of our method

2.1. Spherical harmonics: Background.
Recall first the relation between the cartesian coordinates (x, y, z) and the spherical coordinates (θ, λ), $0 \leq \theta \leq \pi, 0 \leq \lambda < 2\pi$, of a point η on the unit 2-d sphere $\mathbb{S}^2$:

$$(2.1) \qquad \eta = (x, y, z) = (\sin\theta\cos\lambda, \sin\theta\sin\lambda, \cos\theta).$$

Thus θ is the co-latitude (polar distance) and λ is the longitude of the point η. We shall denote by $\xi \cdot \eta$ the inner product of $\xi, \eta \in \mathbb{S}^2$ and by $\rho(\xi, \eta)$ the geodesic distance (angle) between ξ and η. If $\xi, \eta \in \mathbb{S}^2$ are given in spherical coordinates, e.g. $\xi = (\theta', \lambda')$, $\eta = (\theta, \lambda)$, then according to the Spherical Law of Cosines

$$(2.2) \qquad \xi \cdot \eta = \cos\rho(\xi, \eta) = \cos\theta'\cos\theta + \sin\theta'\sin\theta\cos(\lambda' - \lambda).$$

Denote by $\mathcal{H}_n$ ($n \geq 0$) the space of all *spherical harmonics of degree n* on $\mathbb{S}^2$. We refer the reader to [15] and [10] for the basics of spherical harmonics. The standard *orthonormal* basis $\{\tilde{\mathcal{C}}_{m,n}\}_{m=0}^n \cup \{\tilde{\mathcal{S}}_{m,n}\}_{m=1}^n$ for $\mathcal{H}_n$ is defined in terms of the associated Legendre functions of the first kind $P_{m,n}$. Namely, for $\xi = (\theta, \lambda)$

$$(2.3) \qquad \begin{aligned} \tilde{\mathcal{C}}_{m,n}(\xi) &= q_{m,n}P_{m,n}(\cos\theta)\cos m\lambda, \quad m = 0, 1, \cdots, n, \\ \tilde{\mathcal{S}}_{m,n}(\xi) &= q_{m,n}P_{m,n}(\cos\theta)\sin m\lambda, \quad m = 1, 2, \cdots, n, \end{aligned}$$

where the coefficients $q_{m,n}$ are given by

$$(2.4) \qquad q_{0,n} = \sqrt{2n+1}; \quad q_{m,n} = \sqrt{2(2n+1)\frac{(n-m)!}{(n+m)!}}, \quad m = 1, \ldots, n,$$

and

$$P_{m,n}(x) = (1 - x^2)^{m/2}\frac{d^m}{dx^m}P_n(x).$$

Here P_n is the nth degree Legendre polynomial normalized by $P_n(1) = 1$, i.e.

$$(2.5) \qquad P_n(x) = \frac{1}{2^n n!}\frac{d^n}{dx^n}(x^2 - 1)^n.$$

Then for $m = 0, 1, \cdots, n$, $m' = 0, 1, \cdots, n'$ we have

$$\frac{1}{4\pi} \int\limits_{\mathbb{S}^2} \tilde{\mathcal{C}}_{m,n}(\xi) \tilde{\mathcal{C}}_{m',n'}(\xi) \, d\sigma(\xi) = \frac{1}{4\pi} \int\limits_{\mathbb{S}^2} \tilde{\mathcal{S}}_{m,n}(\xi) \tilde{\mathcal{S}}_{m',n'}(\xi) \, d\sigma(\xi) = \delta_{m,m'} \delta_{n,n'},$$

$$(2.6) \qquad \frac{1}{4\pi} \int\limits_{\mathbb{S}^2} \tilde{\mathcal{C}}_{m,n}(\xi) \tilde{\mathcal{S}}_{m',n'}(\xi) \, d\sigma(\xi) = 0,$$

where $\delta_{k,\ell}$ is the Kronecker delta and σ is the standard Lebesgue measure on $\mathbb{S}^2$, which in spherical coordinates (2.1) is given by

$$(2.7) \qquad d\sigma(\xi) = \sin\theta \, d\theta \, d\lambda.$$

In the standard basis (2.3) a spherical polynomial Y_N of degree N is given by its coefficients $\{a_{m,n}, b_{m,n}\}$, i.e.

$$(2.8) \qquad Y_N(\xi) = \sum_{n=0}^{N} \sum_{m=0}^{n} (a_{m,n} \tilde{\mathcal{C}}_{m,n}(\xi) + b_{m,n} \tilde{\mathcal{S}}_{m,n}(\xi)).$$

In sums of this form we shall always assume that the term $b_{0,n} \tilde{\mathcal{S}}_{0,n}(\xi)$ is missing (or, equivalently, $\tilde{\mathcal{S}}_{0,n}(\xi) = 0$). Note that the number of coefficients in (2.8) is $(N+1)^2$.

Denote by Π_N the set of all spherical polynomials of degree N. The spherical polynomials are also known as *band-limited functions* on the sphere. As the restriction to $\mathbb{S}^2$ of any algebraic polynomial in three variables is a spherical polynomials (a linear combination of spherical harmonics) [15, Theorem 2.1, Ch. IV], then

$$(2.9) \qquad f \in \Pi_M, \ g \in \Pi_N \implies fg \in \Pi_{M+N}.$$

This property is standard for polynomials but, in general, it is not true for harmonic functions.

An important property of Legendre polynomials is that the kernel of the orthogonal projector $\text{Proj}_{\mathcal{H}_n} : L_2(\mathbb{S}^2) \to \mathcal{H}_n$ of $L_2(\mathbb{S}^2)$ onto $\mathcal{H}_n$ is given by $(1/4\pi)(2n+1)P_n(\xi \cdot \eta)$, i.e.

$$(2.10) \qquad (\text{Proj}_{\mathcal{H}_n} f)(\xi) = \frac{1}{4\pi} \int\limits_{\mathbb{S}^2} (2n+1) P_n(\xi \cdot \eta) f(\eta) d\sigma(\eta), \quad f \in L_2(\mathbb{S}^2),$$

and hence $P_n(\xi \cdot \eta)$ is in $\mathcal{H}_n$ as a function of η for every $\xi \in \mathbb{S}^2$.

As usual we denote by $L_p(\mathbb{S}^2)$, $1 \le p \le \infty$, the space of functions defined on $\mathbb{S}^2$ with norm

$$\|f\|_{L_p(\mathbb{S}^2)} = \left(\frac{1}{4\pi} \int\limits_{\mathbb{S}^2} |f(\xi)|^p \, d\sigma(\xi) \right)^{1/p}.$$

For $p = \infty$ we shall consider both $L_\infty(\mathbb{S}^2)$ and $C(\mathbb{S}^2)$ with the standard modification to sup-norm and max-norm, respectively.

We shall denote by

$$(2.11) \qquad E_N(f)_{L_p(\mathbb{S}^2)} = \inf_{Y \in \Pi_N} \|f - Y\|_{L_p(\mathbb{S}^2)}$$

the best approximation of $f \in L_p(\mathbb{S}^2)$ from spherical polynomials of degree N.

2.2. The problem of spherical polynomial evaluation.
Here we introduce some notation and state precisely the problems of interest to us in this article.

Problem 1. Given a spherical polynomial Y_N with its coefficients $\{a_{m,n}, b_{m,n}\}$, evaluate $Y_N(\xi_j)$ at arbitrary (scattered) points $\xi_j, j = 1, \ldots, J$, on the sphere $\mathbb{S}^2$ with a prescribed precision $\varepsilon > 0$.

As explained in §1 we split this problem into two sub-problems. For the first sub-problem we need regular grid points on the sphere. Examples of such grids are the sets $\mathcal{X}^{(\tau)} = \{\eta_{k,\ell}^{(\tau)} = (\theta_k^{(\tau)}, \lambda_\ell^{(\tau)})\}$, $\tau = 1, 2$, which for given $K, L \geq 1$ are defined by

$$(2.12) \qquad \theta_k^{(1)} = \frac{\pi}{K}k, \ k = 0, 1, \ldots, K; \ \ \lambda_\ell^{(1)} = \frac{2\pi}{L}\ell, \ \ell = 0, 1, \ldots, L - 1;$$

and

$$(2.13) \qquad \theta_k^{(2)} = \frac{\pi}{K}k - \frac{\pi}{2K}, \ k = 1, 2, \ldots, K; \ \ \lambda_\ell^{(2)} = \frac{2\pi}{L}\ell, \ \ell = 0, 1, \ldots, L - 1.$$

Here in $\mathcal{X}^{(1)}$ we consider only one node for $k = 0$ (the North Pole) and only one node for $k = K$ (the South Pole).

Another example, which can be considered as "regular", is the set $\mathcal{X}^{(3)}$ generated by the zeros u_k of the Kth degree Legendre polynomials P_K ($P_K(u_k) = 0$). In this case we write

$$(2.14) \qquad \theta_k^{(3)} = \arccos u_k, \ k = 1, 2, \ldots, K; \ \ \lambda_\ell^{(3)} = \frac{2\pi}{L}\ell, \ \ell = 0, 1, \ldots, L - 1.$$

The relations between K, L and N above are explained in §3.4.

As explained in the introduction, Problem 1 can be split into two problems:

Problem 2. Given a spherical polynomial Y_N with its coefficients $\{a_{m,n}, b_{m,n}\}$, evaluate $Y_N(\eta)$ at all points η from a regular grid $\mathcal{X}$ on $\mathbb{S}^2$, e.g. the $\mathcal{X}$ given in (2.12), (2.13) or (2.14) with precision not exceeding a given ε (or exactly).

Problem 3. Given the values $Y_N(\eta)$ of a spherical polynomial Y_N at regular grid points $\eta \in \mathcal{X}$, evaluate $Y_N(\xi_j)$ at arbitrary (scattered) points $\xi_j, j = 1, \ldots, J$, on the sphere $\mathbb{S}^2$ with precision ε.

Methods for solving Problem 2 were discussed in the introduction. In the present paper we deal with Problem 3.

2.3. Spherical polynomial evaluation via "father needlets".
"Mother needlets" on the sphere have been developed and used in [11, 12]. For the purposes of evaluation of spherical polynomials it is convenient to use spherical "father needlets", defined as kernels of the form

$$(2.15) \qquad \Lambda_N(u) = \sum_{\nu=0}^{\infty} \hat{a}\left(\frac{\nu}{N}\right)(2\nu + 1)P_\nu(u), \quad u \in [-1, 1],$$

where P_ν is the Legendre polynomial (see (2.10)) and $\hat{a}$ is an admissible cutoff function of type (a) according to Definition 1.1 in [6], namely, for some $\alpha > 0$

$$(2.16) \qquad \hat{a} \in C^\infty[0, \infty); \ \ \hat{a}(t) = 1, \ 0 \leq t \leq 1, \ \text{and} \ \hat{a}(t) = 0, \ t \geq 1 + \alpha.$$

The standard choice of α (used in [11, 12, 6]) is $\alpha = 1$. It is convenient to write $\hat{a}$ as

$$(2.17) \qquad \hat{a}(t) = \hat{a}(\hat{b}, \alpha; t) = \begin{cases} 1, & t \in [0, 1]; \\ \hat{b}((1 + \alpha - t)/\alpha), & t \in [1, 1 + \alpha]; \\ 0, & t \in [1 + \alpha, \infty), \end{cases}$$

where $\hat{b}$ satisfies

$$(2.18) \qquad \hat{b} \in C^S[0, 1], \ \hat{b}(0) = 0, \hat{b}(1) = 1, \hat{b}^{(s)}(0) = \hat{b}^{(s)}(1) = 0, \ s = 1, 2, \ldots, S,$$

for sufficiently large S or $S = \infty$. In this section we use (2.18) only with $S = \infty$. Usually $\hat{b}$ satisfies $0 \leq \hat{b} \leq 1$ (hence $0 \leq \hat{a} \leq 1$), although this condition is not necessary for the theory.

By (2.10) and (2.16) it follows that the operator

$$(2.19) \qquad \widetilde{\mathcal{L}}_N f(\xi) := \frac{1}{4\pi} \int_{\mathbb{S}^2} \Lambda_N(\xi \cdot \eta) f(\eta) \, d\sigma(\eta)$$

has the properties:

$$(2.20) \qquad\qquad\qquad \widetilde{\mathcal{L}}_N f = f \quad \forall f \in \Pi_N;$$

$$(2.21) \qquad\quad \widetilde{\mathcal{L}}_N f \in \Pi_{N_\alpha - 1} \quad \forall f \in L_1(\mathbb{S}^2) \text{ with } N_\alpha = \lceil N + \alpha N \rceil;$$

$$(2.22) \qquad \frac{1}{4\pi} \int_{\mathbb{S}^2} |\Lambda_N(\xi \cdot \eta)| \, d\sigma(\eta) = \frac{1}{2} \int_0^\pi |\Lambda_N(\cos\theta)| \sin\theta \, d\theta \leq \bar{c}, \quad \forall \xi \in \mathbb{S}^2.$$

Here in (2.22) $\bar{c} \geq 1$ is a constant depending only on $\hat{a}$. As is shown in [11, Theorem 3.5] the properties of $\hat{a}$ from (2.16) imply nearly exponential localization of the kernels Λ_N from (2.15):

Theorem 2.1. *Let $\hat{a}$ be a cutoff function satisfying* (2.16) *for some $\alpha > 0$. Then for any $s > 0$ there is a constant $\bar{c}_s$ such that*

$$(2.23) \qquad\qquad |\Lambda_N(\cos\theta)| \leq \bar{c}_s N^2 (1 + N\theta)^{-s}, \quad 0 \leq \theta \leq \pi.$$

Note that Theorem 2.1 with $s = 3$ implies the estimate in (2.22).

The localization of Λ_N can be improved to sub-exponential if one additionally requires that $\hat{a} \in C^\infty[0, \infty)$ have "small" derivatives, i.e. $\hat{a}$ satisfies

$$(2.24) \qquad \|\hat{a}\|_\infty \leq \tilde{c}'', \quad \frac{1}{k!} \|\hat{a}^{(k)}\|_\infty \leq \tilde{c}'' \left(\tilde{c}'[\ln(e + k - 1)]^{1+\beta} \right)^k, \quad k = 1, 2, \ldots$$

for some constants $\beta, \tilde{c}', \tilde{c}'' > 0$. The existence of cutoff functions $\hat{a}$ satisfying simultaneously (2.16) and (2.24) is proved in [6, Theorem 3.1] and under more general conditions in [7, Theorem 2.3]. The sub-exponential decay of the kernels Λ_N can be stated as the following (see [6, Theorem 5.1]):

Theorem 2.2. *Let $\hat{a}$ be an admissible cutoff function satisfying* (2.16) *for some $\alpha > 0$ and* (2.24) *for some constants $\beta, \tilde{c}', \tilde{c}'' > 0$. Then the kernels Λ_N from* (2.15) *satisfy*

$$(2.25) \qquad |\Lambda_N(\cos\theta)| \leq c'' N^2 \exp\left\{ -\frac{c'\beta N\theta}{[\ln(e + N\theta)]^{1+\beta}} \right\}, \quad 0 \leq \theta \leq \pi,$$

where $c' = \tilde{c}' c^*$ for an absolute constant $c^* > 0$, and $c'' > 0$ depending only on $\alpha, \beta, \tilde{c}'$ and $\tilde{c}''$.

In order to make the operator $\widetilde{\mathcal{L}}_N$ from (2.19) convenient for computations we discretize $\widetilde{\mathcal{L}}_N$ by using a cubature formula on $\mathbb{S}^2$. Let $\mathcal{X}$ be a finite set of nodes on $\mathbb{S}^2$, e.g. $\mathcal{X}$ is one of the grids $\mathcal{X}^{(\tau)}$, $\tau = 1, 2, 3$, in §2.2. We shall use cubatures

$$(2.26) \qquad \frac{1}{4\pi} \int_{\mathbb{S}^2} f(\eta) \, d\sigma(\eta) \sim \sum_{\eta \in \mathcal{X}} w_\eta f(\eta)$$

with the properties ($M \in \mathbb{N}$ and a constant $\tilde{c} > 0$)

$$(2.27) \qquad \frac{1}{4\pi} \int_{\mathbb{S}^2} f(\eta) \, d\sigma(\eta) = \sum_{\eta \in \mathcal{X}} w_\eta f(\eta) \quad \forall f \in \Pi_{M-1};$$

$$(2.28) \qquad \sum_{\substack{\eta \in \mathcal{X} \\ \cos\rho_2 \le \xi\cdot\eta \le \cos\rho_1}} |w_\eta| \le \tilde{c} \left(\frac{\cos\rho_1 - \cos\rho_2}{2} + \frac{\sin\rho_1 + \sin\rho_2}{M} + \frac{1}{M^2} \right)$$

for all $\xi \in \mathbb{S}^2$ and $0 \le \rho_1 \le \rho_2 \le \pi$. Note that $4\pi(\cos\rho_1 - \cos\rho_2)/2$ above is the area of the spherical ring between the spherical angles ρ_1 and ρ_2. The boundary of the same region is of total length $2\pi(\sin\rho_1 + \sin\rho_2)$. The last term M^{-2} is necessary for values of ρ_1, ρ_2 close to 0. Note that (2.28) with $\xi = \eta \in \mathcal{X}$ and $\rho_1 = \rho_2 = 0$ implies $|w_\eta| \le \tilde{c}M^{-2}$. Having in mind that (2.27) with $f \equiv 1$ implies $\sum_{\eta \in \mathcal{X}} w_\eta = 1$, we conclude that the number of nodes in $\mathcal{X}$ is at least cM^2. In fact, we shall utilize cubatures with cM^2 nodes. Cubatures satisfying (2.27)–(2.28) are constructed in §3.4.

Applying cubature (2.26) to the integral in (2.19) we get a discrete counterpart to the operator $\widetilde{\mathcal{L}}_N$, namely,

$$(2.29) \qquad \mathcal{L}_N f(\xi) := \sum_{\eta \in \mathcal{X}} w_\eta \Lambda_N(\xi \cdot \eta) f(\eta).$$

Furthermore, the superb localization of the kernel Λ_N, given in Theorem 2.2, suggests that most of the terms in (2.29) are very small and this leads us to the idea of introducing the truncated operator

$$(2.30) \qquad \mathcal{L}_{N,\delta} f(\xi) := \sum_{\substack{\eta \in \mathcal{X} \\ \xi\cdot\eta \ge \cos\delta}} w_\eta \Lambda_N(\xi \cdot \eta) f(\eta),$$

where $\delta > 0$ is a small parameter. Observe that in the above sum η runs only over the nodes in $\mathcal{X}$ which are in a δ-neighborhood of the point ξ.

2.4. **Properties of the discrete operators.** We next record some properties of $\mathcal{L}_N$.

Theorem 2.3. *Let Λ_N be given by (2.15) with $\hat{a}$ satisfying (2.16) for some $\alpha > 0$ and let the cubature (2.26) satisfy (2.27)–(2.28) for some $M \ge N$. Then $\mathcal{L}_N$ given by (2.29) satisfies:*

$$(2.31) \qquad \mathcal{L}_N : C(\mathbb{S}^2) \to C(\mathbb{S}^2) \text{ is a bounded linear operator;}$$

$$(2.32) \qquad \|\mathcal{L}_N\| \le C, \text{ where } C > 0 \text{ is a constant independent of } N;$$

$$(2.33) \qquad \mathcal{L}_N f \in \Pi_{N_\alpha - 1} \quad \forall f \in C(\mathbb{S}^2) \text{ with } N_\alpha = \lceil N + \alpha N \rceil.$$

Moreover, if

$$(2.34) \qquad M \ge N + N_\alpha,$$

then

$$\mathcal{L}_N f = f \quad \forall f \in \Pi_N; \tag{2.35}$$

$$\|f - \mathcal{L}_N f\|_{C(\mathbb{S}^2)} \leq (\|\mathcal{L}_N\| + 1) E_N(f)_{C(\mathbb{S}^2)} \quad \forall f \in C(\mathbb{S}^2). \tag{2.36}$$

Proof. Using (2.29) we get (2.31) with norm

$$\|\mathcal{L}_N\| = \sup_{\xi \in \mathbb{S}^2} \sum_{\eta \in \mathcal{X}} |w_\eta| |\Lambda_N(\xi \cdot \eta)|.$$

In order to bound the above quantity we set $\rho_k = 2^{-k}\pi$, $k = 0, 1, \ldots, K$, with $K = \lceil \log_2 N \rceil$ and $\rho_{K+1} = 0$. Thus $\rho_K \sim 2^{-K} \sim N^{-1}$. Using (2.28) and (2.23) with $s = 3$ we get

$$\|\mathcal{L}_N\| \leq \sup_{\xi \in \mathbb{S}^2} \sum_{k=1}^{K+1} \sum_{\substack{\eta \in \mathcal{X} \\ \cos \rho_{k-1} \leq \xi \cdot \eta \leq \cos \rho_k}} |w_\eta| |\Lambda_N(\xi \cdot \eta)|$$

$$\leq c\tilde{c}\bar{c}_3 \left(\sum_{k=1}^{K} \left(\frac{\cos \rho_k - \cos \rho_{k-1}}{2} + \frac{\sin \rho_k + \sin \rho_{k-1}}{N} + \frac{1}{N^2} \right) N^2 (N2^{-k})^{-3} + 1 \right)$$

$$\leq c\tilde{c}\bar{c}_3 \left(\sum_{k=1}^{K} \left(2^{-2k} + 2^{-k}N^{-1} + N^{-2} \right) N^{-1} 2^{3k} + 1 \right) \leq c\tilde{c}\bar{c}_3,$$

where $c > 0$ is an absolute constant. This proves (2.32). Property (2.33) follows from (2.29), (2.15) and (2.10).

By (2.9), (2.15) and (2.10) we infer that if $f \in \Pi_N$, then $\Lambda_N(\xi \cdot \eta)f(\eta)$ is a spherical polynomial of η of degree $N + N_\alpha - 1$ for every $\xi \in \mathbb{S}^2$. Now, property (2.35) follows from (2.29), (2.27), (2.19) and (2.20). For the proof of (2.36) let Y be given by (2.11) with $p = \infty$. Then

$$\|f - \mathcal{L}_N f\|_{C(\mathbb{S}^2)} \leq \|f - Y\|_{C(\mathbb{S}^2)} + \|Y - \mathcal{L}_N Y\|_{C(\mathbb{S}^2)} + \|\mathcal{L}_N(f - Y)\|_{C(\mathbb{S}^2)},$$

which gives (2.35) on account of (2.31) and (2.35). $\qquad\square$

Note that Theorem 2.3 holds for any C^∞ cutoff function $\hat{a}$ and property (2.24) is not needed. From (2.33), (2.11), (2.36) and (2.32) it follows that

$$E_{N_\alpha - 1}(f)_{C(\mathbb{S}^2)} \leq \|f - \mathcal{L}_N f\|_{C(\mathbb{S}^2)} \leq c E_N(f)_{C(\mathbb{S}^2)}, \tag{2.37}$$

which shows the superb approximation properties of operators $\mathcal{L}_N$.

Some of properties of the operators $\mathcal{L}_{N,\delta}$ read as follows:

Theorem 2.4. *Let Λ_N satisfy*

$$|\Lambda_N(\cos \theta)| \leq \gamma \quad for \quad \delta \leq \theta \leq \pi. \tag{2.38}$$

Then under the assumptions of Theorem 2.3 we have

$$\mathcal{L}_{N,\delta} : C(\mathbb{S}^2) \to L_\infty(\mathbb{S}^2) \text{ is a bounded linear operator}; \tag{2.39}$$

$$\|f - \mathcal{L}_{N,\delta} f\|_{L_\infty(\mathbb{S}^2)} \leq \tilde{c}\gamma \|f\|_{\ell_\infty(\mathcal{X})} \quad \forall f \in \Pi_N; \tag{2.40}$$

$$\|f - \mathcal{L}_{N,\delta} f\|_{L_\infty(\mathbb{S}^2)} \leq (C+1)E_N(f)_{C(\mathbb{S}^2)} + \tilde{c}\gamma \|f\|_{\ell_\infty(\mathcal{X})} \quad \forall f \in C(\mathbb{S}^2), \tag{2.41}$$

where $\tilde{c}$ is the constant from (2.28) and C is from (2.32). If the weights of the cubature (2.26) satisfy $w_\eta \geq 0$, $\eta \in \mathcal{X}$, then (2.40) and (2.41) are true with $\tilde{c} = 1$.

Proof. From (2.38) and (2.28) we get

$$\sum_{\substack{\eta \in \mathcal{X} \\ \xi \cdot \eta < \cos \delta}} |w_\eta| \, |\Lambda_N(\xi \cdot \eta)| \leq \sum_{\substack{\eta \in \mathcal{X} \\ \xi \cdot \eta < \cos \delta}} |w_\eta| \, \gamma \leq \tilde{c} \gamma. \tag{2.42}$$

This along with (2.29)-(2.30) leads to

$$|\mathcal{L}_{N,\delta} f(\xi) - \mathcal{L}_N f(\xi)| \leq \sum_{\substack{\eta \in \mathcal{X} \\ \xi \cdot \eta < \cos \delta}} |w_\eta| \, |\Lambda_N(\xi \cdot \eta)| \, \|f\|_{\ell_\infty(\mathcal{X})} \leq \tilde{c} \gamma \|f\|_{\ell_\infty(\mathcal{X})}.$$

Now Theorem 2.4 follows immediately from Theorem 2.3 and the above estimate.

$\square$

Note that by (2.30) it follows that $\mathcal{L}_{N,\delta} f(\xi)$ is a discontinuous function of ξ, which is a piece-wise spherical polynomial of degree $N_\alpha - 1$.

3. Toward an effective computational method

Theorem 2.4 suggests the main steps in solving effectively Problem 3 from §2.2. For simplicity in this section we assume that the cubature weights are positive, and hence $\tilde{c} = 1$.

According to (2.40) with $f = Y_N$ the error of computing (approximating) $Y_N(\xi)$ by means of $\mathcal{L}_{N,\delta} Y_N(\xi)$ will not exceed ε if

$$\gamma = \varepsilon / \|Y_N\|_{\ell_\infty(\mathcal{X})}. \tag{3.1}$$

The quantity $\|Y_N\|_{\ell_\infty(\mathcal{X})}$ can be easily computed as the values $Y_N(\eta)$, $\eta \in \mathcal{X}$, are known. In (3.1) we may consider ε as the absolute error of our method (if the computations are performed in the exact arithmetic), while γ is the relative error (with respect to the polynomial norm, not a particular polynomial value!).

Apparently, the number of operations needed to compute $\mathcal{L}_{N,\delta}(\xi)$ is a constant multiple of the number of terms in (2.30), which in turn depends on how smaller δ is. Thus varying $\hat{a}$ in (2.16) we seek for a given γ the smallest possible δ such that (2.38) holds. Upper and lower bounds for the order of the best possible δ are given in §3.1 and an improved criterion for determining δ is given in §3.2. Note that the choice of δ is independent of the cubature formula (because $\|Y_N\|_{\ell_\infty(\mathcal{X})} \leq \|Y_N\|_{C(\mathbb{S}^2)}$) and its dependence on the polynomial Y_N is very loose; it is only via the polynomial norm and degree.

The problem for fast and accurate computation of the values $\Lambda_N(\xi \cdot \eta)$ is nontrivial due to fact that the function $\Lambda_N(\cos \rho)$ in (2.30) is very rapidly changing its values for ρ close to 0. Thus the round-off error in the computation of $\xi \cdot \eta$ by (2.2) may cause undesirable big error in the value of $\Lambda_N(\xi \cdot \eta)$. In §3.3 we present an effective solution to this problem combined with a very fast method for evaluation of $\Lambda_N(\cos \rho)$.

Having obtained δ we need to determine effectively the nodes $\eta \in \mathcal{X}$ that satisfy $\xi \cdot \eta \geq \cos \delta$. This step gives advantage to nodal sets with some kind of structure, e.g. as in (2.12), (2.13) or (2.14). The values of the cubature weights associated with these nodes and the proof that the cubatures satisfy (2.27)–(2.28) are given in §3.4. In §3.5 we establish for the cubatures from §3.4 sharp error estimate for the truncated operator $\mathcal{L}_{N,\delta}$.

As was pointed out in §2.2 the nodes in (2.12), (2.13) or (2.14) get denser around the poles. This means that for ξ close to one of the poles the sum in (2.30) will

have $O(N^2\delta)$ terms as opposed to the normal $O(N^2\delta^2)$ terms for ξ away from the poles. A simple method for avoiding this undesirable drawback is given in §3.6.

The connection between the cubature and the polynomial degree N is only one-sided – via the inequalities $M > N$ or $M \geq N+N_\alpha$ in the hypothesis of Theorem 2.3. This means that we can increase the degree of exactness M and thus the number of nodes. If we keep δ fixed, then this will lead to higher number of nodes in the δ-neighborhood of ξ and slower computations. Such dependence is inconsistent with the general perception that the knowledge of the polynomial values at larger number of nodes should make the point-wise evaluation easier and faster. In our method in accordance with this idea we can increase the parameter α in (2.16), which will lead to the decrease of δ and, as a consequence, to smaller number of nodes in the δ-neighborhood of a point. The details are given in §3.7.

All elements of our algorithm for solving Problem 3 are given in §3.8.

3.1. **Bounds on δ.** Given $\alpha > 0$, a cutoff function $\hat{a}$ satisfying (2.16), $0 < \gamma \leq 1$ and $N \geq 1$ we denote by

$$\delta(\hat{a}; \gamma, N)$$

the minimal δ for which (2.38) holds. We next derive lower and upper bounds on $\delta(\hat{a}; \gamma, N)$.

For the lower bound we shall employ the Chebyshev polynomials. By (2.15)–(2.16) it follows that Λ_N (defined in (2.15)) is an algebraic polynomial of degree $n = N_\alpha - 1$ satisfying

$$(3.2) \qquad \Lambda_N(1) = \sum_{\nu=0}^{n} \hat{a}\left(\frac{\nu}{N}\right)(2\nu+1) \approx C(\hat{a})N^2$$

with $1 \leq C(\hat{a}) \leq (1+\alpha)^2$. As is well known among all algebraic polynomials of degree n, which are bounded by 1 on $[-1,1]$, the Chebyshev polynomial of the first kind T_n has the fastest growth for $u > 1$. Therefore, the n-th degree polynomial $\tilde{T}_n(u) = \gamma T_n((2u+d)/(2-d))$ with $d = 1-\cos\delta_0$ satisfies the counterpart of (2.38), namely,

$$|\tilde{T}_n(\cos\theta)| \leq \gamma \quad \text{for} \quad \delta_0 \leq \theta \leq \pi \quad \text{provided} \quad \tilde{T}_n(1) = \Lambda(1).$$

From this condition, (3.2) and the standard representation of $T_n(u)$ for $u \geq 1$ we obtain the following equation for δ_0

$$(3.3) \qquad \left(t+\sqrt{t^2-1}\right)^n + \left(t-\sqrt{t^2-1}\right)^n = \frac{2C(\hat{a})N^2}{\gamma}, \quad t = \frac{3-\cos\delta_0}{1+\cos\delta_0}.$$

Thus we have proved

Proposition 3.1. *For any $\hat{a}, \gamma, N$ as above we have $\delta(\hat{a}; \gamma, N) \geq \delta_0$, where δ_0 is determined in* (3.3).

The exact explicit solution of (3.3) is not possible, but the asymptotic of δ_0 for large N and small γ is readily available:

$$(3.4) \qquad \delta_0 \approx \frac{\sqrt{2}}{1+\alpha} \frac{\ln(2C(\hat{a})N^2/\gamma)}{N}.$$

This asymptotic formula gives a clear idea what is the best that can be expected from $\delta(\hat{a}; \gamma, N)$. However, the lower bound on $\delta(\hat{a}; \gamma, N)$ from Proposition 3.1 is hardly achievable since the first N coefficients of Λ_N in the Legendre polynomial

basis (determined by $\hat{a}$) behave much differently compared to the coefficients of $\tilde{T}_n$ in the same basis.

Due to a possible rapid growth of the constants $\{\bar{c}_s\}$ in Theorem 2.1 conditions (2.16) on $\hat{a}$ (used as hypothesis in Theorem 2.3) solely are not sufficient for obtaining a good upper bound on $\delta(\hat{a}; \gamma, N)$. Cutoff functions $\hat{a}$ with "small" derivatives as in (2.24), however, come to the rescue.

Proposition 3.2. *Let $N \in \mathbb{N}$ and $\alpha, \beta, \gamma > 0$. Assume $\hat{a}$ obeys (2.16) and (2.24) with the given α and β. Let the constants $c', c'' > 0$ be from (2.25) and let the constant $E_\beta > 0$ be defined by*

$$(3.5) \qquad E_\beta := \sup_{u \geq 0} \left[\frac{\ln(e + u[\ln(e + u)]^{1+\beta})}{\ln(e + u)} \right]^{1+\beta}.$$

Then for $\gamma < c'' N^2$ we have $\delta(\hat{a}; \gamma, N) \leq \delta_1$ with

$$(3.6) \qquad \delta_1 := \frac{E_\beta}{c'\beta} \frac{\ln(c''N^2/\gamma)}{N} \left[\ln \left(e + \frac{E_\beta}{c'\beta} \ln(c''N^2/\gamma) \right) \right]^{1+\beta}.$$

Proof. From (3.5) with $u = \frac{E_\beta}{c'\beta} \ln(c''N^2/\gamma) > 0$ and (3.6) it follows that

$$\frac{c'\beta N\delta_1}{[\ln(e + N\delta_1)]^{1+\beta}} \geq \ln(c''N^2/\gamma).$$

From (2.25) and the above inequality we get for every $\theta \in [\delta_1, \pi]$

$$|\Lambda_N(\cos\theta)| \leq c''N^2 \exp\left\{ -\frac{c'\beta N\theta}{[\ln(e + N\theta)]^{1+\beta}} \right\}$$

$$\leq c''N^2 \exp\left\{ -\frac{c'\beta N\delta_1}{[\ln(e + N\delta_1)]^{1+\beta}} \right\} \leq c''N^2 \exp\left\{ -\ln(c''N^2/\gamma) \right\} = \gamma,$$

which proves the proposition. $\qquad\square$

Neglecting the constants in (3.6) for large N^2/γ we arrive at

$$(3.7) \qquad \delta_1 \leq c \frac{\ln(N^2/\gamma)}{N} \left[\ln\ln(N^2/\gamma) \right]^{1+\beta}.$$

Thus the difference between estimates (3.4) and (3.7) is a double logarithmic factor, which is essentially a constant for the values of the parameters considered here; the quantities $\ln\ln(N_1^2/\gamma_1)$ with $N_1 = 10^3$, $\gamma_1 = 10^{-6}$, and $\ln\ln(N_2^2/\gamma_2)$ with $N_2 = 10^4$, $\gamma_2 = 10^{-8}$, differ from one another with less than 10%.

3.2. **An improved criterion for δ.** The majorant of $|\Lambda_N(\cos\theta)|$ given by (2.25), after reaching the value γ for $\theta = \delta_1$, preserves its fast decay for $\theta > \delta_1$. This means that it is possible to select a smaller value of δ in (2.30) and still have the same error bound. This can be achieved, for example, by replacing the uniform condition in (2.38) by an integral one. Thus we arrive at the equation

$$(3.8) \qquad \frac{1}{2} \int_{-1}^{\cos\delta} |\Lambda_N(x)|\, dx = \frac{\gamma}{2} \left| \int_{-1}^{1} \Lambda_N(x)\, dx \right| = \gamma,$$

which determines $\delta = \bar{\delta}(\hat{a}; \gamma, N)$ as a function of γ, N and $\hat{a}$ (satisfying (2.16) for some $\alpha > 0$). The fact that the second integral in (3.8) is equal to 2 follows from (2.15) and the orthogonality of Legendre polynomials.

Equation (3.8) is justified by the following approximate identity (see (2.42)) for cubatures *with positive weights*:

$$(3.9) \qquad \sum_{\substack{\eta \in \mathcal{X} \\ \xi \cdot \eta < \cos \delta}} w_\eta \, |\Lambda_N(\xi \cdot \eta)| \cong \frac{1}{4\pi} \int_{\xi \cdot \eta < \cos \delta} |\Lambda_N(\xi \cdot \eta)| \, d\sigma(\eta)$$

$$= \frac{1}{4\pi} \int_\delta^\pi |\Lambda_N(\cos \theta)| \sin \theta \, d\theta \int_0^{2\pi} 1 \, d\lambda = \frac{1}{2} \int_{-1}^{\cos \delta} |\Lambda_N(x)| \, dx = \gamma.$$

From (2.38) and (3.8) we get immediately

$$(3.10) \qquad \bar{\delta}(\hat{a}; \gamma, N) \leq \delta(\hat{a}; \gamma, N).$$

Hence, the upper bound from Proposition 3.2 holds for $\bar{\delta}(\hat{a}; \gamma, N)$ as well. However, using (2.25) this upper bound can be improved as follows:

Theorem 3.3. *Assume that for a given $\hat{a}$ the kernels Λ_N satisfy (2.25) for some $c', c'', \beta > 0$, $\beta \leq 1$. Then there exists a number $C_1 > 0$ depending only on c', c'' and β such that for any $N \in \mathbb{N}$ and $0 < \gamma \leq e^{-e}$ we have $\bar{\delta}(\hat{a}; \gamma, N) \leq \delta_2$, where*

$$(3.11) \qquad \delta_2 := C_1 \frac{\ln(1/\gamma)}{N} \left[\ln \ln(1/\gamma) \right]^{1+\beta}.$$

For convenience we place the proof of Theorem 3.3 in §3.5.

From (3.9) and Theorem 3.3 we get the following error bound on the truncated operator

$$(3.12) \qquad \| \mathcal{L}_N f - \mathcal{L}_{N,\delta} f \|_{L_\infty(\mathbb{S}^2)} \leq \gamma \| f \|_{\ell_\infty(\mathcal{X})} \quad \forall f \in \Pi_N$$

for every $\delta \in [\delta_2, \pi]$ with δ_2 given in (3.11). We shall prove estimate (3.12) for the cubatures from §3.4 independently of (3.9) in §3.5 (see Theorem 3.12).

Note that for a fixed γ the upper bound for $\bar{\delta}(\hat{a}; \gamma, N)$ in (3.11) with the increase of N becomes smaller than the lower bound for $\delta(\hat{a}; \gamma, N)$ in Proposition 3.1. This fact justifies the replacement of (2.38) in Theorem 2.4 by (3.8) for practical application. Note that the product $N\delta_2$ depends on γ but not on N. This means that the complexity of (2.30) will not depend on N and we can use $\mathcal{L}_{N,\delta}$ for very high degrees N.

Looking for small δ in (2.30) we arrived at

Problem 4. For given $\alpha > 0$, $\gamma \in (0,1]$ and $N \geq 1$ find a cutoff function $\hat{a}$ satisfying (2.16) which minimizes $\bar{\delta}(\hat{a}; \gamma, N)$.

In Problem 4 we can relax the requirement $\hat{a} \in C^\infty$ without changing its essence. In making $\bar{\delta}(\hat{a}; \gamma, N)$ as small as possible we necessarily look for cutoff functions $\hat{a}$ with high smoothness and "small" derivatives.

Selection of $\hat{a}$. For fixed $\hat{a}$, γ and N it is easy to write code for approximate computation of $\bar{\delta}(\hat{a}; \gamma, N)$ from (3.8) and thus to compare its values for different $\hat{a}$. Although this is not a solution of Problem 4, it guided us in selecting for our purposes cutoff functions $\hat{a}(\hat{b}_n, \alpha; t)$ of the form (2.17) with $n = 5, 6$, where $\hat{b}_n$ is defined by

$$\hat{b}_n(u) := \frac{(2n+1)!!}{2(2n)!!} \int_0^{\pi u} \sin^{2n+1} t \, dt = \frac{1}{2} - \frac{\cos \pi u}{2} - \frac{\cos \pi u}{2} \sum_{k=1}^n \frac{(2k-1)!!}{(2k)!!} \sin^{2k} \pi u.$$

Note that the functions $\hat{b}_n(v/\pi)$ are trigonometric polynomials of degree 11 or 13, respectively, and $\hat{b}'_n(v/\pi)$ has zeros of order $2n+1$ at 0 and at π. Here it is important that the values of $\hat{b}_n(v/\pi)$ can be computed rapidly at many points with sufficiently high precision. The values of $\bar{\delta}(\hat{a}; \gamma, N)$ for $\hat{a}$ defined by (2.17) with $\alpha = 3$ and $\hat{b} = \hat{b}_5$ and for several choices of N and γ are given in Table 2 in §5.

A better choice for $\hat{a}$ could be the cutoff function $\hat{a}$ with "small" derivatives (see (2.24)) from [6, Theorem 3.1]. However, as for now we do not have a practical algorithm which allows to quickly compute the values of that $\hat{a}$ at many points with sufficiently high precision.

3.3. Accurate kernel evaluation.
The next step in developing our algorithm is the accurate and fast evaluation of $\Lambda_N(\xi \cdot \eta)$ for given $\xi, \eta \in \mathbb{S}^2$, which is a nontrivial task.

For every $u \in [-1, 1]$ one can evaluate $\Lambda_N(u)$ using, for instance, the downward Clenshaw recurrence formula. It employs the Legendre recurrence relation

$$(n+1)P_{n+1}(u) = (2n+1)uP_n(u) - nP_{n-1}(u), \quad n \geq 0; \quad P_0(u) = 1, \; P_{-1}(u) = 0.$$

This algorithm is numerically stable and fast since it requires $O(N)$ operations.

The straightforward calculation of $\Lambda_N(\xi \cdot \eta)$, where $u = \xi \cdot \eta$ is obtained via (2.2) and $\Lambda_N(u)$ is computed by the Clenshaw summation, looses accuracy when ξ is close to η that is exactly the case we are interesting in. In order to improve the accuracy by several significant digits we perform the calculations as follows:

(i): We compute the spherical distance ρ between $\xi = (\theta', \lambda')$ and $\eta = (\theta, \lambda)$ via the Haversine Law of Spherical Trigonometry

$$(3.13) \qquad \sin^2 \frac{\rho}{2} = \sin^2 \frac{\theta' - \theta}{2} + \sin \theta' \sin \theta \sin^2 \frac{\lambda' - \lambda}{2}.$$

(ii): We compute $\Lambda_N(\xi \cdot \eta) = (\Lambda_N \circ \cos)(\rho)$ via an approximation of $\Lambda_N \circ \cos$.

The Haversine Law (3.13) is well-conditioned for computation of ρ close to 0 and the round-off error is smaller when compared with the Spherical Law of Cosines (2.2). This fact has been known since the XIX century. The haversine function is defined by $\operatorname{hav} t := (1 - \cos t)/2 = \sin^2(t/2)$; we have used the last form in (3.13).

The advantage of using the trigonometric polynomial $\Lambda_N \circ \cos$ in step (ii) over the algebraic polynomial Λ_N stems from the fact that the derivative of $\Lambda_N \circ \cos$ near the origin is cN times smaller than the derivative of Λ_N near 1.

In order to get fast and accurate evaluation of $(\Lambda_N \circ \cos)(\rho)$ for $\rho \in [0, \delta]$ we take the equally spaced points $t_r = \delta r/R$ for $r = -s, -s+1, \ldots, R+s$ and determine $t_r^* = \arccos(\cos t_r)$. Note that in general $t_r^* \neq t_r$ because of the machine arithmetic, while $\cos t_r^*$ and $\cos t_r$ coincide as double precision numbers. Then $\Lambda_N(u_r)$, determined for $u_r = \cos t_r = \cos t_r^*$ via the Clenshaw summation, is a good approximation to $(\Lambda_N \circ \cos)(t_r^*)$. Thus we have the values of $\Lambda_N \circ \cos$ at the points t_r^*, which are close to equally spaced but not equally spaced. Now $(\Lambda_N \circ \cos)(\rho)$ is computed by Lagrange interpolation of $\Lambda_N \circ \cos$ with nodes t_r^*, $r = m-s, m-s+1, \ldots, m+s+1$, where $m = \lfloor \rho R/\delta \rfloor$. The Lagrange polynomial is of degree $2s + 1$.

The choice of R and s depends on the targeted relative error γ and the degree $N_\alpha - 1$ of $\Lambda_N \circ \cos$. Our experiments showed that for $\gamma \geq 10^{-10}$ and $N_\alpha \leq 16000$ one can take $R = 2000$ and $s = 1$ or $s = 2$. The numbers $\Lambda_N(u_r)$ are computed in $O(NR)$ operations and stored at the initial stage of the program. At the later stages the evaluation of $(\Lambda_N \circ \cos)(\rho)$ requires only $O(s)$ operations. Of course, the

third degree Lagrange interpolation, i.e. $s = 1$, is faster but less accurate than the fifth degree Lagrange interpolation for $s = 2$.

The graph of the kernel $\Lambda_N \circ \cos$ in $[0, \delta]$ as well its extrema and their location in this interval are given in Figure 3 and Table 3 in §5.

3.4. **Nodes and cubatures.** The following lemma gives a simple method for constructing cubatures on $\mathbb{S}^2$ from one-dimensional quadratures. These simple cubatures are very attractive since they are exact for high degree spherical polynomials and their nodes and weights can be computed easily to very high precision. They also demonstrate the advantage of the regular grids defined in §2.2 over other "regular" grids such as HEALPix.

Lemma 3.4. *Let $K, L \geq 1$ and assume that the quadrature*

$$(3.14) \qquad \frac{1}{2} \int_{-1}^{1} f(t)\, dt \sim \sum_{k=0}^{K} v_k f(u_k),$$

with $u_k \in [-1, 1]$ is exact for all algebraic polynomials of degree $K_1 - 1$ and the quadrature

$$(3.15) \qquad \frac{1}{2\pi} \int_{0}^{2\pi} g(t)\, dt \sim \sum_{\ell=0}^{L-1} \bar{v}_\ell g(\lambda_\ell),$$

with $\lambda_\ell \in [0, 2\pi)$ is exact for all trigonometric polynomials of degree $L_1 - 1$. Then the cubature

$$(3.16) \qquad \frac{1}{4\pi} \int_{\mathbb{S}^2} F(\xi)\, d\sigma(\xi) \sim \sum_{k=0}^{K} \sum_{\ell=0}^{L-1} v_k \bar{v}_\ell F(\arccos(u_k), \lambda_\ell)$$

is exact for all spherical polynomials of degree $M - 1$ with $M = \min\{K_1, L_1\}$.

The lemma is immediate from the form of the basis of $\mathcal{H}_n$ given in (2.3) (with the variables separated) and the form of the measure $d\sigma$ given in (2.7).

Note that if $u_k = 1$, then all nodes $(\arccos(u_k), \lambda_\ell) = (0, \lambda_\ell)$ coincide with the North Pole and the cubature weight associated with this node is $v_k = \sum_{\ell=0}^{L-1} v_k \bar{v}_\ell$. A similar modification is made if $u_k = -1$, i.e the node coincides with the South Pole.

The case of quadrature (3.15) is quite simple, the best choice is the rectangular quadrature

$$(3.17) \qquad \frac{1}{2\pi} \int_{0}^{2\pi} g(t)\, dt \sim \sum_{\ell=0}^{L-1} \frac{1}{L} g(\lambda_\ell), \quad \lambda_\ell = \frac{2\pi}{L}\ell,\ \ell = 0, \ldots, L-1,$$

which is exact for trigonometric polynomials of degree $L - 1$.

The algebraic quadrature formulas (3.14) with nodes $\{\cos\theta_k^{(\tau)}\}$, $\tau = 1, 2, 3$, from §2.2 are given in the following three lemmas.

Lemma 3.5. *For given $K \geq 1$ denote by $u_k^{(1)} = \cos\theta_k^{(1)}$, $\theta_k^{(1)} = \pi k/K$, $k = 0, 1, \ldots, K$, the points of extrema of the Chebyshev polynomial T_K. If the weights*

$\{v_k^{(1)}\}$ *are defined by*

$$(3.18) \quad v_0^{(1)} = v_K^{(1)} := \frac{1}{2K(2R+1)},$$

$$v_k^{(1)} := \frac{1}{K}\left(\frac{1}{2R+1} + 4\sum_{r=1}^{R}\frac{\sin^2 r\theta_k^{(1)}}{4r^2-1}\right), \quad k = 1,\dots,K-1,$$

where $R = \lfloor (K-1)/2 \rfloor$, *then the quadrature*

$$(3.19) \qquad \frac{1}{2}\int_{-1}^{1} f(t)\,dt \sim \sum_{k=0}^{K} v_k^{(1)} f(u_k^{(1)}),$$

is exact for all algebraic polynomials of degree $2\lfloor (K+1)/2 \rfloor - 1 \geq K - 1$.

Lemma 3.6. *Given* $K \geq 1$ *denote by* $u_k^{(2)} = \cos\theta_k^{(2)}$, $\theta_k^{(2)} = \pi(2k-1)/(2K)$, $k = 1,\dots,K$, *the zeros of the Chebyshev polynomial* T_K. *If the weights* $\{v_k^{(2)}\}$ *are defined by*

$$(3.20) \qquad v_k^{(2)} := \frac{1}{K}\left(\frac{1}{2R+1} + 4\sum_{r=1}^{R}\frac{\sin^2 r\theta_k^{(2)}}{4r^2-1}\right), \quad k = 1,\dots,K,$$

where $R = \lfloor (K-1)/2 \rfloor$, *then the quadrature*

$$(3.21) \qquad \frac{1}{2}\int_{-1}^{1} f(t)\,dt \sim \sum_{k=1}^{K} v_k^{(2)} f(u_k^{(2)}),$$

is exact for all algebraic polynomials of degree $2\lfloor (K+1)/2 \rfloor - 1 \geq K - 1$.

Quadrature (3.19) is usually known as Clenshaw–Curtis quadrature [1] or Fejér's second quadrature. (In [4, 5] Fejér gave the values of $v_k^{(1)}$ under the assumption that $f(-1) = f(1) = 0$.) Quadrature (3.21) is usually known as Fejér's first quadrature [4, 5]. The weight expressions (3.18), (3.20) deviate from the standard ones, but we prefer them because they underline the weights' positivity.

Lemma 3.7. *For* $K \geq 1$ *denote by* $u_k^{(3)} = \cos\theta_k^{(3)}$, $\theta_k^{(3)} \in (0,\pi)$, $k = 1,\dots,K$, *the zeros of the Legendre polynomial* P_K. *If the weights* $\{v_k^{(3)}\}$ *are defined by*

$$(3.22) \qquad v_k^{(3)} := \left(P_K'(\cos\theta_k^{(3)})\sin\theta_k^{(3)}\right)^{-2}, \quad k = 1,\dots,K,$$

then the Gaussian quadrature

$$(3.23) \qquad \frac{1}{2}\int_{-1}^{1} f(t)\,dt \sim \sum_{k=1}^{K} v_k^{(3)} f(u_k^{(3)}),$$

is exact for all algebraic polynomials of degree $2K - 1$.

There are several effective schemes of complexity $O(K)$ (logarithmic factors are omitted) for computing with good precision the values of the nodes and weights $\theta_k^{(3)}, v_k^{(3)}$ of the Gaussian quadratures. We shall not elaborate on them.

Applying (3.17) and Lemmas 3.5–3.7 in Lemma 3.4 we get

Theorem 3.8. *Let $M \geq 1$ and assume that $\mathcal{X}^{(\tau)}$, $\tau = 1, 2, 3$, is one of the regular grids from §2.2 with $K, L \geq 1$ satisfying the conditions*

$$(3.24) \qquad M \leq L, \qquad M \leq \begin{cases} 2 \lfloor (K+1)/2 \rfloor, & \tau = 1, 2; \\ 2K, & \tau = 3. \end{cases}$$

For $\eta = (\theta_k^{(\tau)}, \lambda_\ell^{(\tau)}) \in \mathcal{X}^{(\tau)}$ set $w_\eta^{(\tau)} = v_k^{(\tau)} L^{-1}$. Then the cubature

$$(3.25) \qquad \frac{1}{4\pi} \int_{\mathbb{S}^2} F(\xi) \, d\sigma(\xi) \sim \sum_{\eta \in \mathcal{X}^{(\tau)}} w_\eta^{(\tau)} F(\eta)$$

is exact for all spherical polynomials of degree $M - 1$.

In other words, if $K \geq M$ and $L \geq M$, then we have a cubature satisfying (2.27) with nodes at the regular grid points from (2.12) or (2.13). It a number of applications we have $L \approx 2K$ because at the equator the mesh size is $2\pi/L$ in the longitude direction and π/K in the latitude direction. For the grid points (2.14) the condition $K \geq M$ may be relaxed to $K \geq M/2$.

Our next step is to show that the cubatures from Theorem 3.8 satisfy (2.28). To this end for any finite set $\mathcal{X} \subset \mathbb{S}^2$ we define the Voronoi cells Ω_η, $\eta \in \mathcal{X}$, by

$$\Omega_\eta = \{\xi \in \mathbb{S}^2 \; : \rho(\xi, \eta) \leq \rho(\xi, \zeta) \;\; \forall \zeta \in \mathcal{X}\},$$

i.e. Ω_η consists of all points from the sphere, which are closer to η than to any other point from $\mathcal{X}$. Note that every cell is a convex spherical polygon. The set of all Voronoi cells forms the Voronoi tessellation of $\mathbb{S}^2$. Thus $\cup_{\eta \in \mathcal{X}} \Omega_\eta = \mathbb{S}^2$ and the interiors of any two different cells are disjoint.

The connection between the Voronoi tessellation and (2.28) is given by

Lemma 3.9. *Let for some constants $\tilde{c}', \tilde{c}''$ the weights of cubature (2.26) satisfy $|w_\eta| \leq \tilde{c}'|\Omega_\eta|$ ($|\Omega_\eta|$ is the Lebesgue measure of Ω_η) and $\mathrm{diam}(\Omega_\eta) \leq \tilde{c}'' M^{-1}$ for all $\eta \in \mathcal{X}$. Then the cubature satisfies (2.28).*

Proof. Let $\xi \in \mathbb{S}^2$ and $0 \leq \rho_1 \leq \rho_2 \leq \pi$. We denote by $\mathcal{X}(\xi, \rho_1, \rho_2)$ the set of all $\eta \in \mathcal{X}$ such that $\cos \rho_2 \leq \xi \cdot \eta \leq \cos \rho_1$. Set $\bar{\rho}_1 = \max\{\rho_1 - \tilde{c}'' M^{-1}, 0\}$ and $\bar{\rho}_2 = \min\{\rho_2 + \tilde{c}'' M^{-1}, \pi\}$. Evidently, $\Omega_\eta \subset \{\zeta \in \mathbb{S}^2 \; : \; \cos \bar{\rho}_2 \leq \xi \cdot \zeta \leq \cos \bar{\rho}_1\}$ for all $\eta \in \mathcal{X}(\xi, \rho_1, \rho_2)$. Hence

$$\sum_{\eta \in \mathcal{X}(\xi, \rho_1, \rho_2)} |w_\eta| \leq \tilde{c}' \Big| \bigcup_{\eta \in \mathcal{X}(\xi, \rho_1, \rho_2)} \Omega_\eta \Big| \leq \tilde{c}' \int_{\cos \bar{\rho}_2 \leq \xi \cdot \zeta \leq \cos \bar{\rho}_1} 1 \, d\sigma(\zeta)$$

$$= 2\pi \tilde{c}' (\cos \bar{\rho}_1 - \cos \bar{\rho}_2)$$

and the lemma follows. $\qquad \square$

Now it is easy to prove

Theorem 3.10. *Under the hypothesis of Theorem 3.8 the cubature (3.25) satisfies (2.28).*

Proof. For the Gaussian quadrature ($\tau = 3$) it is well known that uniformly

$$(3.26) \quad \theta_{k+1}^{(3)} - \theta_k^{(3)} \sim K^{-1}, \; k = 1, 2, \ldots, K-1, \quad \theta_1^{(3)} \sim K^{-1}, \quad \pi - \theta_K^{(3)} \sim K^{-1}.$$

Using also $\lambda_{\ell+1}^{(3)} - \lambda_\ell^{(3)} = 2\pi L^{-1}$ we get $\text{diam}(\Omega_\eta) = O(\max\{K^{-1}, L^{-1}\}) = O(M^{-1})$ and $|\Omega_\eta| \sim K^{-1}L^{-1}\sin\theta_k^{(3)}$. The weights $v_k^{(3)}$ are positive and satisfy uniformly (see e.g. [13])

$$(3.27) \qquad v_k^{(3)} \sim K^{-1}\sin\theta_k^{(3)}, \quad k = 1, 2, \ldots, K,$$

which implies $w_\eta^{(3)} \leq \tilde{c}'|\Omega_\eta|$. Now Lemma 3.9 proves the theorem in the case $\tau = 3$.

If $\tau = 1$ or $\tau = 2$ we have estimates similar to (3.26) and (3.27). Estimate (3.27) follows from (3.18) and (3.20), and (3.26) follows from (2.12) and (2.13). The only exceptions are the two poles ($k = 0$ and $k = K$) in the case $\tau = 1$. If η is any of them, we have $|\Omega_\eta| \sim K^{-2}$ and $w_\eta^{(1)} = K^{-1}(2\lfloor(K-1)/2\rfloor + 1)^{-1}$. This completes the proof. $\qquad\square$

Theorem 3.8 and Theorem 3.10 show that cubatures (3.25) satisfy (2.27) and (2.28) under the assumptions (3.24). Consequently, if (2.34) is fulfilled, then the operators from (2.29) and (2.30) satisfy Theorem 2.3 and Theorem 2.4, respectively, for every of the cubatures (3.25).

We now turn our attention to the problem for determining the nodes $\eta = (\theta, \lambda) \in \mathcal{X}^{(\tau)}$, which satisfy $\xi \cdot \eta \geq \cos\delta$ for given $\xi = (\theta', \lambda') \in \mathbb{S}^2$ and $\delta \in (0, \pi/2]$. From the Law of Sines in spherical trigonometry we conclude that for $\delta \leq \theta' \leq \pi - \delta$ it suffices to have

$$(3.28) \qquad (\theta, \lambda) \in [\theta' - \delta, \theta' + \delta] \times [\lambda' - \phi, \lambda' + \phi], \quad \phi = \arcsin(\sin\delta/\sin\theta').$$

For $0 \leq \theta' < \delta$ (3.28) can be replaced by $(\theta, \lambda) \in [0, \theta' + \delta] \times [0, 2\pi)$ and for $\pi - \delta < \theta' \leq \pi$ by $(\theta, \lambda) \in [\theta' - \delta, \pi] \times [0, 2\pi)$. It is easy to create code which determines quickly the indices of the grid points $\eta = (\theta_k, \lambda_\ell)$ satisfying (3.28). Observe that approximately $\pi/4$ of the grid points obeying (3.28) satisfy $\xi \cdot \eta \geq \cos\delta$. Thus, if the kernel is evaluated for all grid points satisfying (3.28), then the extra work of 27.4% could be fully compensated by not performing the verification $\xi \cdot \eta \geq \cos\delta$.

The number of points from $\mathcal{X}^{(\tau)}$, $\tau = 1, 2, 3$, satisfying (3.28) is approximately

$$(3.29) \qquad \nu = \frac{2KL\delta^2}{\pi^2\sin\theta'}.$$

Thus the number of terms in (2.30) increases from $O(KL\delta^2)$ for points at the equator to $O(KL\delta)$ for points near the poles. This drawback of our method can easily be overcome as shown in §3.6.

3.5. Truncation error estimate for the cubatures from §3.4.
In this subsection we prove Theorem 3.3 and show in Theorem 3.12 below that for the cubatures from §3.4 inequality (3.12) holds for δ of the form (3.11).

For $\beta > 0$ set

$$(3.30) \qquad \Phi_\beta(t) = c'' \exp\left\{-\frac{c'\beta t}{[\ln(e+t)]^{1+\beta}}\right\}, \quad t \in [0, \infty),$$

where c' and c'' are the constants from (2.25). Then estimate (2.25) in Theorem 2.2 takes the form

$$(3.31) \qquad |\Lambda_N(\cos\theta)| \leq N^2\Phi_\beta(N\theta), \quad 0 \leq \theta \leq \pi.$$

The following lemma will be instrumental in the proof of Theorem 3.3.

Lemma 3.11. *Let $c', c'' > 0$, $0 < \beta \leq 1$. Then there exists a constant $C_1 > 0$ depending only on c', c'' and β such that for any $0 < \gamma \leq e^{-e}$ and*

$$(3.32) \qquad T := C_1 \ln(1/\gamma) \left[\ln \ln(1/\gamma)\right]^{1+\beta}$$

we have

$$(3.33) \qquad \frac{1}{2} \int_T^\infty \Phi_\beta(t) t \, dt \leq \gamma.$$

Proof. Set $g(t) := c'\beta t [\ln(e+t)]^{-1-\beta}$. Then

$$\frac{tg'(t)}{g(t)} = 1 - \frac{t(1+\beta)}{(e+t)\ln(e+t)}$$

and hence

$$(3.34) \qquad \frac{1}{3} \leq \frac{tg'(t)}{g(t)} \leq 1 \qquad \forall t \geq 0.$$

Thus g is strictly increasing. Using

$$\frac{d}{dt} \frac{t^2}{g(t)} = \frac{t}{g(t)} \left(2 - \frac{tg'(t)}{g(t)}\right)$$

and (3.34) it follows that

$$(3.35) \qquad \frac{t}{g(t)} \leq \frac{d}{dt} \frac{t^2}{g(t)} \leq \frac{5}{3} \frac{t}{g(t)} \qquad \forall t \geq 0.$$

Now, from (3.35) and (3.34) we get for any $T > 0$

$$\int_T^\infty \exp\{-g(t)\} \frac{t^2}{g(t)} g'(t) \, dt = - \int_T^\infty \frac{t^2}{g(t)} \, d\exp\{-g(t)\}$$

$$= \frac{T^2}{g(T)} \exp\{-g(T)\} + \int_T^\infty \exp\{-g(t)\} \frac{d}{dt} \frac{t^2}{g(t)} \, dt$$

$$\leq \frac{T^2}{g(T)} \exp\{-g(T)\} + \frac{5}{3} \int_T^\infty \exp\{-g(t)\} \frac{t}{g(t)} \, dt$$

$$\leq \frac{T^2}{g(T)} \exp\{-g(T)\} + 5 \int_T^\infty \exp\{-g(t)\} \frac{t^2 g'(t)}{g(t)^2} \, dt.$$

Hence

$$(3.36) \qquad \int_T^\infty \exp\{-g(t)\} \frac{t^2}{g(t)} g'(t) \left(1 - \frac{5}{g(t)}\right) dt \leq \frac{T^2}{g(T)} \exp\{-g(T)\}.$$

Assume

$$T \geq C_2 := \frac{20 E_\beta}{c'\beta} \left[\ln\left(e + \frac{20 E_\beta}{c'\beta}\right)\right]^{1+\beta},$$

where E_β is the constant defined in (3.5). Then from (3.5) with $u = \frac{20E_\beta}{c'\beta}$ it follows that $g(t) \geq 20$ for $t \geq T$. Hence, (3.30), (3.34) and (3.36) yield

$$\int\limits_T^\infty \Phi_\beta(t)t\,dt \leq 3\int\limits_T^\infty c'' \exp\{-g(t)\}\,\frac{t^2}{g(t)}g'(t)\,dt \leq 4c''\frac{T^2}{g(T)}\exp\{-g(T)\}.$$

Therefore,

$$\frac{1}{2}\int\limits_T^\infty \Phi_\beta(t)t\,dt \leq \frac{2c''}{c'\beta}T[\ln(e+T)]^{1+\beta}\exp\left\{-\frac{c'\beta T}{[\ln(e+T)]^{1+\beta}}\right\}$$

$$(3.37) \qquad\qquad \leq \frac{2c''}{c'\beta}\exp\left\{-\frac{(1/2)c'\beta T}{[\ln(e+T)]^{1+\beta}}\right\}$$

for $T \geq C_3$, where C_3 is sufficiently large, depending only on c' and β ($C_3 \geq C_2$). It is readily seen that estimate (3.37) with T as in (3.32) with C_1 sufficiently large (depending only on c', c'', and β) implies (3.33). $\qquad\square$

Now Theorem 3.3 is an easy consequence of Lemma 3.11.

Proof of Theorem 3.3. Given $N \in \mathbb{N}$ and $0 < \gamma \leq e^{-e}$ set $\delta_2 := N^{-1}T$, where T is defined as in (3.32). Then by (3.31) and Lemma 3.11 we have

$$\frac{1}{2}\int\limits_{-1}^{\cos\delta_2} |\Lambda_N(x)|\,dx = \frac{1}{2}\int\limits_{\delta_2}^\pi |\Lambda_N(\cos u)|\sin u\,du$$

$$\leq \frac{1}{2}\int\limits_{\delta_2}^\pi N^2\Phi_\beta(Nu)\sin u\,du = \frac{1}{2}\int\limits_T^\infty \Phi_\beta(t)t\,dt \leq \gamma.$$

On account of (3.8) the above implies Theorem 3.3. $\qquad\square$

We next show that inequality (3.12) can be established in a slightly weaker form for the cubatures from §3.4 without making use of the approximate identity (3.9).

Theorem 3.12. *Let $N \in \mathbb{N}$ and $\alpha > 0$, $0 < \beta \leq 1$. Assume $\hat{a}$ obeys (2.16) and (2.24) with the given α and β. Let the cubature (3.25) with nodes $\mathcal{X} = \mathcal{X}^{(\tau)}$ and weights $w_\eta = w_\eta^{(\tau)}$, $\tau = 1, 2, 3$, fulfill the hypothesis of Theorem 3.8 with M satisfying (2.34). Then there exist numbers $\widetilde{C}_1, \widetilde{C}_2 > 0$ depending only on α, β, the constants c', c'' from Theorem 2.2 and the constants $\tilde{c}', \tilde{c}''$ from Lemma 3.9 such that for all $0 < \gamma \leq \widetilde{C}_2$ and $\delta \in [\delta_3, \pi]$ we have*

$$(3.38) \qquad \sum_{\substack{\eta \in \mathcal{X} \\ \xi\cdot\eta < \cos\delta}} w_\eta\,|\Lambda_N(\xi\cdot\eta)| \leq \gamma,$$

where

$$(3.39) \qquad \delta_3 := \widetilde{C}_1\frac{\ln(1/\gamma)}{N}\,[\ln\ln(1/\gamma)]^{1+\beta}.$$

As a consequence estimate (3.12) holds with $\delta = \delta_3$.

Proof. From (2.16), (2.24) and Theorem 2.2 we obtain that the kernel Λ_N satisfies (2.25) and hence (3.31). From (2.34) we get $M \geq (2+\alpha)N$. According to Theorem 3.10 the cubature (3.25) satisfies Lemma 3.9 and hence

$$(3.40) \qquad |w_\eta| \leq \tilde{c}'|\Omega_\eta|, \quad \mathrm{diam}(\Omega_\eta) \leq \tilde{c}''M^{-1} \quad \forall \eta \in \mathcal{X},$$

where Ω_η is the Voronoi cell for $\eta \in \mathcal{X}$. Set

$$D_{\alpha,\beta} := \sup_{t \in [0,\infty)} \Phi_\beta(t)/\Phi_\beta(t + \tilde{c}''/(2+\alpha)) = \exp\left\{\beta c'\tilde{c}''/(2+\alpha)\right\}.$$

Using the triangle inequality, (3.40) and (2.34) we get

$$N\rho(\xi,\zeta) \leq N\rho(\xi,\eta) + \tilde{c}''/(2+\alpha) \quad \text{for} \quad \zeta \in \Omega_\eta$$

and, hence, for all $\xi \in \mathbb{S}^2$, $\eta \in \mathcal{X}$ and $\zeta \in \Omega_\eta$ we have

$$(3.41) \qquad \Phi_\beta(N\rho(\xi,\eta)) \leq D_{\alpha,\beta}\Phi_\beta\big(N\rho(\xi,\eta) + \tilde{c}''/(2+\alpha)\big) \leq D_{\alpha,\beta}\Phi_\beta(N\rho(\xi,\zeta)).$$

Now from (3.40), (3.31), (3.41) and Lemma 3.11 with $\gamma/(4\pi\tilde{c}'D_{\alpha,\beta})$ instead of γ we get for $\gamma \leq 4\pi\tilde{c}'D_{\alpha,\beta}e^{-e}$

$$\sum_{\substack{\eta \in \mathcal{X} \\ \xi\cdot\eta < \cos\delta}} w_\eta\,|\Lambda_N(\xi\cdot\eta)| \leq \tilde{c}' \sum_{\substack{\eta \in \mathcal{X} \\ \xi\cdot\eta < \cos\delta}} \int_{\Omega_\eta} 1\,d\sigma(\zeta)\,N^2\Phi_\beta(N\rho(\xi,\eta))$$

$$\leq \tilde{c}'D_{\alpha,\beta}N^2 \sum_{\substack{\eta \in \mathcal{X} \\ \xi\cdot\eta < \cos\delta}} \int_{\Omega_\eta} \Phi_\beta(N\rho(\xi,\zeta))\,d\sigma(\zeta)$$

$$\leq \tilde{c}'D_{\alpha,\beta}N^2 \int_{\xi\cdot\zeta < \cos(\delta - \tilde{c}''M^{-1})} \Phi_\beta(N\rho(\xi,\zeta))\,d\sigma(\zeta)$$

$$= 2\pi\tilde{c}'D_{\alpha,\beta}N^2 \int_{\delta - \tilde{c}''M^{-1}}^{\pi} \Phi_\beta(N\theta)\sin\theta\,d\theta$$

$$\leq \frac{4\pi\tilde{c}'D_{\alpha,\beta}}{2} \int_{N\delta - \tilde{c}''NM^{-1}}^{\infty} \Phi_\beta(t)t\,dt$$

$$\leq 4\pi\tilde{c}'D_{\alpha,\beta}\frac{\gamma}{4\pi\tilde{c}'D_{\alpha,\beta}} = \gamma$$

provided

$$N\delta \geq C_1 \ln(4\pi\tilde{c}'D_{\alpha,\beta}/\gamma)\left[\ln\ln(4\pi\tilde{c}'D_{\alpha,\beta}/\gamma)\right]^{2+2\beta} + \tilde{c}''/(2+\alpha).$$

Taking the constant $4\pi\tilde{c}'D_{\alpha,\beta}$ out of the logarithms in the above inequality we get that (3.38) holds for every $\delta \in [\delta_3, \pi]$ with δ_3 given in (3.39). $\qquad\square$

Theorem 3.12 has mainly theoretical value showing that the operator $\mathcal{L}_{N,\delta_3}$ can be used for spherical polynomial evaluation with δ_3 from (3.39). The practical value of the theorem is diminished by the fact that the constant $\widetilde{C}_1$ is too large.

Note also that Theorem 3.12 holds for all cutoff functions $\hat{a}$ obeying (2.16) and (2.24). This might be considered as positive information because many cutoff functions can be applied in computations. However, the theorem lacks the criterion property of the approximate identity (3.9) as it does not show which of two given cutoff functions will guarantee the aimed precision with less operations.

3.6. **Computations near the poles.** In order to evaluate $\mathcal{L}_{N,\delta}f(\xi)$ at points $\xi = (\theta', \lambda')$ with latitudes between 45° North and 45° South, i.e. $\pi/4 \leq \theta' \leq 3\pi/4$, we apply the method as explained so far. For the remaining points from the two 45° caps centered at the poles we apply the change of variables

$$(3.42) \qquad x = \tilde{z}, \;\; y = \tilde{x}, \;\; z = \tilde{y},$$

or in spherical coordinates

$$(\sin\theta\cos\lambda, \sin\theta\sin\lambda, \cos\theta) = (\cos\tilde{\theta}, \sin\tilde{\theta}\cos\tilde{\lambda}, \sin\tilde{\theta}\sin\tilde{\lambda}).$$

In the new coordinate system the above spherical caps appear as 45° caps centered at the points $(\pi/2, \pi/2)$ and $(\pi/2, 3\pi/2)$, which are on the new equator. In order to apply the same operator we need the values of the spherical polynomial to be approximated at regular grid points with respect to the new coordinate system, which are its values at the images of these grid points under the mapping inverse to (3.42). Note that each of the spaces $\mathcal{H}_n$, $n = 0, 1, 2, \ldots$, is invariant under the mapping (3.42) (rotation).

Using this approach we essentially improve the computational speed for points near the poles. Now in the worst case scenario one uses a factor of $\sqrt{2}$ more points to evaluate $\mathcal{L}_{N,\delta}f(\xi)$ than the points used when ξ is on the equator. Another positive feature is the reduction of the total number of nodes where we have to precompute the polynomial values. The reduction is by approximately 25% and is due to the fact that the grid points, which are denser near the poles, are replaced by new points with "equatorial" density.

3.7. **Optimal selection of parameters.** For a given function $\hat{b}$ satisfying (2.18) let $\hat{a} = \hat{a}(\hat{b}, \alpha)$ be defined by (2.17). Here we focus out attention on the following problem:

Suppose a spherical polynomial of degree N is given by its values at, say, the $M \times 2M$ regular grid points (2.13). Choose α subject to (2.34) so that the number of terms in (2.30) is minimal.

To be more specific, let, say, $N = 1000$, $M = 6000$, $\gamma = 10^{-8}$ and $\delta = \tilde{\delta}_\alpha = \bar{\delta}(\hat{a}; \gamma, N)$ as in §3.2. Consider the following two selections of α:

   (i): $\alpha = 4$ in the definition of $\hat{a}$ and we make the computations using $\tilde{\delta}_4$ and the 6000×12000 grid ($M = 6000$);
   (ii): $\alpha = 1$ in the definition of $\hat{a}$ and we make the computations using $\tilde{\delta}_1$ and the 3000×6000 sub-grid ($M = 3000$). Of course, we can use a larger sub-grid, but this will lead only to higher number of terms.

The question is, in which case the cap $\{\xi \cdot \eta \geq \cos\delta\}$ will contain less points from the respective grid.

Note that (2.34) is satisfied as equality in both cases. This makes us to define $M := N(2 + \alpha)$ which is the best choice for the grid parameter. The number of grid points in the δ-neighborhood of a point is a constant multiple of $(M\delta)^2 = ((2 + \alpha)N\delta_\alpha)^2$.

Without going into details we would like to mention the asymptotic equality

$$(3.43) \qquad \tilde{\delta}_\alpha \cong \frac{C(\gamma, \alpha)}{N\alpha}$$

valid for a fixed $\hat{b}$. In fact, $C(\gamma, \alpha)$ in (3.43) is a slowly varying function of γ and $\alpha \geq \alpha_0$, which has a limit as $\alpha \to \infty$.

Thus the number of terms is $c(1 + 2\alpha^{-1})^2$, which is a decreasing function of α. In particular, this result implies that the smallest number of terms for given N and M will be achieved for the largest possible α in (2.34), i.e. we cannot gain speed by using sub-grids. Going back to our example, in case (i) we have approximately 4 times less terms than in case (ii).

3.8. **The algorithm.** Based on the ideas from §2 and §3 we propose the following algorithm for solving Problem 3:

(1) Choose a function $\hat{b}$ with "small" derivatives which satisfies (2.18) for large S or $S = \infty$ (see §3.2).
(2) Using (3.18), (3.20) or (3.22) determine the weights $w_\eta^{(\tau)}$, $\tau = 1, 2, 3$, of the cubature (3.25) according to the type τ of the grid $\mathcal{X}^{(\tau)}$ from §2.2.
(3) Determine the largest possible M for the cubature.
(4) For the given M, N determine the largest possible α satisfying (2.34).
(5) Determine $\|Y_N\|_{\ell_\infty(\mathcal{X})}$ and γ from (3.1).
(6) For $\hat{a}$ given by (2.17) determine $\hat{a}(\nu/N)$.
(7) Determine $\delta = \bar{\delta}(\hat{a}; \gamma, N)$ from (3.8).
(8) For $\hat{a}$ and δ from Steps 6–7 compute $\Lambda_N(\cos t_r^*)$, $r = -s, -s+1, \ldots, R+s$ (see §3.3).
(9) For every $\xi_j, j = 1, \ldots, J$, compute $Y_N(\xi_j)$ using (2.30) with $f = Y_N$, where $\Lambda_N(\xi_j \cdot \eta) = (\Lambda_N \circ \cos)(\rho)$ is determined as in §3.3 with ρ determined from (3.13).

If the improvement described in §3.6 is applied, then for every $\xi_j, j = 1, \ldots, J$, in Step 9 one verifies in advance to which of the three domains ξ_j belongs and in two of the three cases the change of variables (3.42) is applied before computing the approximation in (2.30).

We next determine the complexity of all steps in the typical case $K = O(N)$, $L = O(N)$. Step 2 requires $O(N \log N)$ operations when FFT is used for computing $v_k^{(\tau)}$ and $O(N^2)$ assignments to $w_\eta^{(\tau)}$. In Step 5 we need $O(N^2)$ operations. The values $\hat{a}(\nu/N)$ in Step 6 can be computed in $O(N \log \deg \hat{b}_n)$ operations using the representation in §3.2 and the computation of δ in Step 7 can be done with good precision with $O(N^2)$ operations. In Step 8 we need $O(NR)$ operations. The total complexity of the preparatory Steps 1–8 is $O(N^2)$ without counting the operations necessary to compute $Y_N(\eta)$, $\eta \in \mathcal{X}^{(\tau)}$ (or the time to read them from the disk).

From inequalities (3.29) and (3.11) we get that the number of terms in (2.30) is $O([\ln(1/\varepsilon)]^2 [\ln\ln(1/\varepsilon)]^{2+2\beta})$ (or $O([\ln(N^2/\varepsilon)]^2 [\ln\ln(N^2/\varepsilon)]^{2+2\beta})$ if criterion (2.38) is applied). Hence, $O(J [\ln(1/\varepsilon)]^2 [\ln\ln(1/\varepsilon)]^{2+2\beta})$ is the total complexity of Step 9.

4. GENERALIZATIONS AND APPLICATIONS

4.1. **Generalization to higher dimensions.** Let $\mathbb{S}^d$ $(d \geq 1)$ be the unit sphere in $\mathbb{R}^{d+1}$ and denote by $\mathcal{H}_\nu$ $(\nu \geq 0)$ the space of all spherical harmonics of degree ν on $\mathbb{S}^d$. It is well known [15, p. 140] that $\dim \mathcal{H}_\nu^d = \frac{(2\nu+d-1)\Gamma(\nu+d-1)}{\Gamma(d)\Gamma(\nu+1)}$ for $\nu \geq 1$ and $\dim \mathcal{H}_0^d = 1$.

As is well known [15] the orthogonal projector $\mathrm{Proj}_{\mathcal{H}_\nu} : L_2(\mathbb{S}^d) \to \mathcal{H}_\nu$ has the representation (a generalization of (2.10))

$$(4.1) \qquad (\mathrm{Proj}_{\mathcal{H}_\nu} f)(\xi) = \frac{1}{\omega_d} \int_{\mathbb{S}^d} \frac{\nu + \kappa}{\kappa} C_\nu^\kappa(\xi \cdot \eta) f(\eta) d\sigma(\eta),$$

where σ is the standard Lebesgue measure on $\mathbb{S}^d$, $\kappa := \frac{d-1}{2}$, $\omega_d := \int_{\mathbb{S}^d} 1 d\sigma = \frac{2\pi^{\kappa+1}}{\Gamma(\kappa+1)}$ is the hypersurface area of $\mathbb{S}^d$, and $\xi \cdot \eta$ stands for the inner product of $\xi, \eta \in \mathbb{S}^d$. Here C_ν^κ is the Gegenbauer polynomial of degree ν normalized with $C_\nu^\kappa(1) = \binom{\nu+2\kappa-1}{\nu}$ [3, p. 174].

Using the relationship between Gegenbauer and Jacobi polynomials [17, (4.7.1)]

$$C_\nu^\kappa(t) = \frac{\Gamma(\kappa+1/2)}{\Gamma(2\kappa)} \frac{\Gamma(\nu+2\kappa)}{\Gamma(\nu+\kappa+1/2)} P_\nu^{(\kappa-1/2,\kappa-1/2)}(t)$$

we obtain the following generalization of (2.15)

$$(4.2) \qquad \Lambda_N(t) = \sum_{\nu=0}^\infty \hat{a}\left(\frac{\nu}{N}\right) \frac{(\nu+\kappa)\Gamma(\kappa+1/2)\Gamma(\nu+2\kappa)}{\kappa\Gamma(2\kappa)\Gamma(\nu+\kappa+1/2)} P_\nu^{(\kappa-1/2,\kappa-1/2)}(t).$$

In dimension $d = 1$ one has after passing to the limit in (4.1) and (4.2) as $\kappa \to 0$ (here $F = f \circ \cos$)

$$(\mathrm{Proj}_{\mathcal{H}_\nu} F)(\varphi) = \frac{1}{2\pi} \int_0^{2\pi} (2 - \delta_{\nu,0}) \cos\nu(\varphi - \theta) F(\theta) d\theta,$$

$$\Lambda_N(t) = \sum_{\nu=0}^\infty \hat{a}\left(\frac{\nu}{N}\right)(2 - \delta_{\nu,0}) T_\nu(t),$$

where T_ν is the ν-th degree Chebyshev polynomial and $\delta_{n,m}$ is the Kronecker delta.

The point is that in the general case all necessary ingredients are either known, e.g. the generalization of the sub-exponential decay of Λ_N in Theorem 2.2 is proved in [6, Theorem 5.1], or can be derived following the same route as when $d = 2$. Let us only mention that estimate (3.11) remains true. Hence, the number of terms in (2.30) becomes $O([\ln(1/\varepsilon)]^d [\ln\ln(1/\varepsilon)]^{d+d\beta})$.

Finally, let us point out that in the case $d = 1$ our method serves as an algorithm for fast evaluation of trigonometric polynomials at scattered points.

4.2. **Working with grids of wider mesh size.** There are two groups of conditions important to our theory: (a) inequalities (3.24) connecting K and L with M, and (b) deg $Y_N \leq N$ and inequality (2.34) connecting M with N. The first group can be consider as a simple definition of the term "spherical degree of exactness M". For simplicity in this subsection we consider the case of equally spaced nodes (with $L = 2K = 2M$), so the distance between the nodes is π/M in both latitude and longitude direction (at the equator).

We now turn our attention to the group (b) conditions. Let $\widetilde{N} = \deg Y_N$ be the exact degree of the polynomial to be evaluated. The condition $\widetilde{N} \leq N$ is implicitly part of our theory, however, in applications one can choose in (2.15) $N < \widetilde{N}$. Similarly, condition (2.34) was essentially used in establishing (2.35) in Theorem 2.3 and (2.40) in Theorem 2.4, which enable us to claim that the error of approximation does not exceed ε. In the typical case $\alpha = 1$, however,

inequality (2.34) implies $M \geq 3N$, i.e. the nodes are at least three times denser (linearly) than the the sampling interval for the Nyquist frequency π/N for Nth degree polynomials. Therefore, the fundamental question here is:

Can one utilize successfully the truncated operators from (2.30) whenever (A) $N < \widetilde{N}$ and/or (B) $M < (2 + \alpha)N$?

We would like to emphasize that we are interested in significant reductions of the sizes of N and M above. A small percentage reductions of N and M are always possible since the coefficients $\hat{a}(\nu/N)$ of Λ_N are very close to 1 when ν is close to N and very small when ν is close to N_α. Also the trivial positive answer of question (B) that (2.30) is applicable for $M > 2N$ (with $\bar{\alpha} = MN^{-1} - 2$) is not very satisfactory. Of course, one will be covered by the theory but, as explained in §3.7, decreasing α reduces significantly the speed of the algorithm.

One can write explicitly the errors which conditions (A) and (B) bring in property (2.35). Effects of such type are often called "aliasing". These questions can also be explored numerically when taking γ smaller than the aliasing error. One of the conclusions from our experiments in Example 1 in §5 is that condition (A) is more damaging to the error than condition (B) for polynomials with *nonvanishing* coefficients $a_{m,n}, b_{m,n}$ for n closed to $\widetilde{N}$.

The above question has a positive answer in the the case when (i) one has to compute the values of a spherical polynomial Y_N which approximates a function with a given smoothness (i.e. Y_N has certain smoothness), and (ii) the error must not exceed ε which is within some reasonable bound depending on the smoothness of Y_N (not arbitrarily small). Being able to reduce significantly the size of M allows to utilize our method for fast compressed (memory efficient) evaluation of spherical polynomials with tight control on the accuracy. This is precisely the case described in Example 2 in §5.

4.3. **Application to other problems.** The operators $\mathcal{L}_N$ from (2.29) and their truncated versions $\mathcal{L}_{N,\delta}$ in (2.30) are a powerful *approximation tool* as evidenced by estimates (2.36) in Theorem 2.3 and (2.41) in Theorem 2.4. Note that condition (2.34) is no longer needed when these operators are used for approximation. Rather, the identity $N = M/(2 + \alpha)$ can be used to define the parameter N appearing in the right-hand sides of (2.36) and (2.41).

The superb localization of the kernels of the operators $\mathcal{L}_N$ and $\mathcal{L}_{N,\delta}$ and their compatibility with spherical harmonics make them an excellent tool for global as well as local approximation. The latter is a desirable feature for practical applications. Here "local" means that the approximant is closer to the approximated function in regions where the function is smoother than globally. This is a well known fact in the classical approximation theory.

Formulas (2.29) and, especially, (2.30) can be viewed as "interpolation" formulas, and hence used for *fast generation of surfaces in computer-aided geometric design*.

Our algorithm can also be used for *fast verification* whether given data represent (within accuracy ε) the values at given regular grid points of some spherical polynomial of a given degree N. The criterion is defined by

$$|f(\xi) - \mathcal{L}_{N,\delta}f(\xi)| \leq \varepsilon \quad \forall \xi \in \mathcal{X},$$

where $f(\xi)$ denotes the value at ξ and δ is calculated for γ defined in (3.1). In this case the grid should be oversampled with respect to the polynomial degree.

As already indicated the algorithm considered in this paper is based on the spherical "father needlets". For other purposes we have also developed algorithms for approximation and representation of functions on the sphere based on the "mother needlets" introduced in [11, 12], which are similar in nature to the widely used wavelets. We shall not present the details of that development here.

5. Numerical experiments

The method for evaluation of high degree spherical polynomials at scattered points described in this article has been implemented in software written in MAT-LAB 7.2 with double-precision variables. Variable precision arithmetic has not been used in the code.

All our experiments were conducted in real time on a standard 1.6 GHz PC with 1 GB of RAM. The method has been intensively tested for degrees between 500 and 2160. The verification of experiments with high degree spherical polynomials is not easy for lack of independent reliable software. For instance, the MATLAB function `legendre(n,X,'norm')` gives wrong answers (including 0 or NaN) for degrees $n > 3000$.

We have also made a number of experiments with spherical polynomials of degrees up to 8000 and compared the results with the results of code performing sharp direct computations in variable precision arithmetic. Unfortunately, such code is too slow for any substantial testing. In all experiments the results were in full agreement with the theory.

Here we report the result of two experiments with our method: the first with spherical polynomials of "large" high degree coefficients, and the second with the spherical polynomial representing the geoid undulation in the 2160 model of NGA (EGM2160) with relatively small high degree coefficients.

**Example 1.** For $n = 500$, $n = 1000$ and $n = 2000$ let F_n be defined by

$$F_n(\theta, \lambda) := q_{0,n} P_{0,n}(\cos \theta) + 2 \sum_{m=1}^{n} q_{m,n} P_{m,n}(\cos \theta) \cos(m\lambda)$$

with $q_{m,n}$ given by (2.4). The values of F_n on an 800×1600 grid range from -452.1885 to 371.7888; F_n has values close to zero in the interiors of the domains $\{(\theta, \lambda) : 0 < \theta < \frac{\pi}{2}, \frac{\pi}{2} < \lambda < \frac{3\pi}{2}\}$ and $\{(\theta, \lambda) : \frac{\pi}{2} < \theta < \pi, -\frac{\pi}{2} < \lambda < \frac{\pi}{2}\}$. The extrema of F_n are localized around $(\frac{\pi}{2}, \frac{\pi}{2})$ and $(\frac{\pi}{2}, \frac{3\pi}{2})$. The graph of F_{500} in spherical coordinates is given in Figure 1.

A representative of the behavior of F_n is the region $\mathcal{D} = \{(\theta, \lambda) : |\frac{\pi}{2} - \theta| \leq \frac{\pi}{15}, |\pi - \lambda| \leq \frac{2\pi}{15}\}$, where we have high oscillation in the longitude direction and essential decrease of the absolute value in the latitude direction. The values of F_n in $\mathcal{D}$ range from -22.7986 to 22.8061. The graph of F_n over this rectangle is given in Figure 2.

Our experiments have shown full agreement of the test results with the theory. The error of computation was within the prescribed bound ε for $\varepsilon = 10^{-5}$, 10^{-6}, 10^{-7}, 10^{-8}, 10^{-9}, 10^{-10} in all cases, whereas γ in (3.1) was determined by $\|F_{500}\|_{\ell_\infty} = 450$ for $\xi \in [0, \pi] \times [0, 2\pi)$ and by $\|F_{500}\|_{\ell_\infty} = 23$ for $\xi \in \mathcal{D}$. The later increase of γ is allowed by the local nature of the operators.

Experiments with parameters satisfying conditions (A) and/or (B) of §4.2 showed that for $\varepsilon = 10^{-10}$ practically no significant reduction of speed is possible. On the other hand a gain of speed by a factor of two is possible for $\varepsilon = 10^{-5}$ (depending
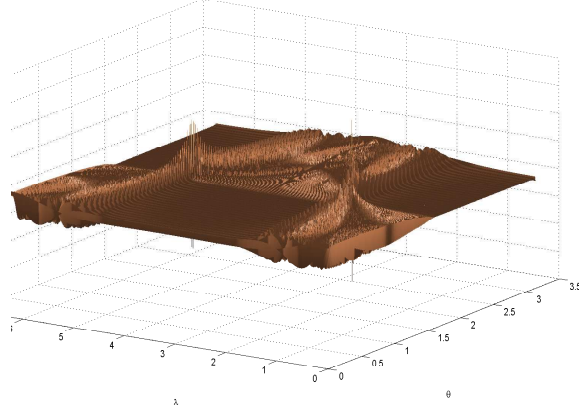
FIGURE 1. Graph of F_{500}
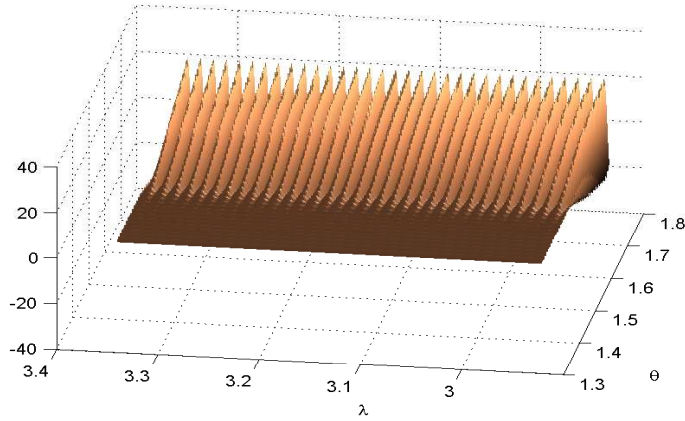
FIGURE 2. Graph of F_{500} over $\mathcal{D}$

on the number of grid points). Under similar ratios in conditions (A) and (B) the contribution of condition (A) to the error was higher than the contribution of condition (B).

The behavior of F_n for $n = 1000$ and $n = 2000$ is the same.

Example 2. The geoid undulation G is approximated by a spherical polynomial of degree and order $\widetilde{N} = 2159$, computed in the official Earth Gravitational Model EGM2008 and publicly released by the U.S. National Geospatial-Intelligence Agency (NGA). The polynomial coefficients have been taken from

http://earth-info.nga.mil/GandG/wgs84/gravitymod/egm2008/egm08_wgs84.html.

This website also contains the values of the geoid undulation on two mesh grids of type (2.12): $2.5' \times 2.5'$ (i.e. $K = M = 4320$, $L = 8640$) and $1' \times 1'$ (i.e. $K = M = 10800$, $L = 21600$). The $1' \times 1'$ grid points are $233, 301, 600$. The geoid

undulation values as single precision numbers occupy 890MB on the hard disk and range from $-106.9\ m$ to $85.8\ m$.

The table given below summarizes the results of the testing. The following programs are compared:

- `hsynth_WGS84` – the NGA spherical harmonic synthesis program computing G by its coefficients directly from (2.8); written in FORTRAN; for comparison purposes assumed to be exact, so the error is 0.
- `interp_1min` – the NGA spherical harmonic synthesis program computing G by spline interpolation of the $1' \times 1'$ undulation data; written in FOR-TRAN; because of the higher memory requirements, the code was tested on a different computer (with larger RAM) to avoid paging.
- `interp_2p5min` – the NGA spherical harmonic synthesis program computing G by spline interpolation of the $2.5' \times 2.5'$ undulation data; written in FORTRAN.
- `needlet3` – implementation of our algorithm which uses the $3' \times 3'$ undulation data; written in MATLAB.
- `needlet4` – implementation of our algorithm which uses the $4' \times 4'$ undulation data; written in MATLAB.

Program	Size HD (MB)	Size RAM (MB)	points/ second	Error (mm)
hsynth_WGS84	71.2	53.9	2	0
interp_1min	890.0	1814.0	80000	0.37
interp_2p5min	142.5	287.6	79280	2.42
needlet3	70.9	132.4	1000	0.10
needlet4	41.1	100.2	400	0.17

Table 1: Program comparison by memory size, speed and error

The NGA program `interp_2p5min` requires approximately 16 seconds to be loaded into the memory and initialized, while each of `needlet3` or `needlet4` requires approximately 3 seconds. The total run time should be formed as the sum of these values plus the time for proper point evaluation computed using column "points/second" above.

Program `hsynth_WGS84` solves Problem 1 while the remaining programs solve Problem 3 described in §2.2.

The sampling interval for the Nyquist frequency is $\pi/2160 = 5'$ and programs `needlet3` and `needlet4` work with $3' \times 3'$ and $4' \times 4'$ mesh grids producing results with relative errors approximately $\gamma = 10^{-6}$. The programs demonstrate that for some quantities used in practice one can violate (2.34) as discussed in §4.2 and still achieve very good approximation. As explained before one can increase the accuracy of the needlet software by simply increasing δ without doing computations for new grid points, which is not the case with the spline interpolation software `interp_1min` and `interp_2p5min`.

The test results described in Table 1 show that `needlet3` and `needlet4` are memory efficient and, therefore, they can be effectively used for fast compressed and accurate computation of the geoid undulation at scattered points on the sphere. This is the main advantage of `needlet3` and `needlet4` over `interp_1min`. Of course, as usual here there is a trade-off between memory size and speed.

Observe also that we use the same algorithm for both Example 1 and Example 2. In contrast, the spline interpolation software discussed above is inadequate for evaluating functions as in Example 1 because of their rapid oscillation.

In the rest of this section we give the numeric values of some parameters used in our algorithm and the form of the kernel Λ_N.

We begin with the values of $\bar{\delta}(\hat{a}; \gamma, N)$ (§3.2) for several selections of N and γ. Here $\hat{a}$ is defined in (2.17) with $\alpha = 3$ and $\hat{b} = \hat{b}_5$ given in §3.2.

$\gamma \setminus N$	500	1000	2000	4000	8000	# nodes
10^{-5}	0.02644	0.013222	0.006611	0.003306	0.0016528	1 391
10^{-7}	0.03546	0.017729	0.008865	0.004432	0.0022162	2 501
10^{-9}	0.05039	0.025195	0.012599	0.006302	0.0031551	5 052

Table 2: The values of $\bar{\delta}(\hat{a}; \gamma, N)$ for $\alpha = 3$
and number of nodes from a $M \times M$ grid, $M = (2 + \alpha)N$

The last column above indicates the number of points from the $M \times M$ grid ($M = (2 + \alpha)N$) in the $\bar{\delta}$-neighborhood of a point at the Equator; it is computed from $((2 + \alpha)N\bar{\delta}/\pi)^2 \pi$ and indicates the number of terms in (2.30) for ξ at the Equator. For a general $\xi = (\theta', \lambda')$ this number has to be divided by $\sin \theta'$. The number is valid for the mesh grids from (2.12) and (2.13), while for (2.14) it has to be divided by 2.

The graph of the kernel $\Lambda_N \circ \cos$ in $[0, \delta]$ is given in Figure 3, while Table 3 contains its extrema and their locations on $[0, \delta]$. The values of the parameters are $N = 1000$, $\hat{a}$ is defined by (2.17) with $\alpha = 3$ and $\hat{b} = \hat{b}_5$ given in §3.2 and $\gamma = 10^{-6}$.

| Abscissa	Value	Abscissa	Value
0	$6.3283 \cdot 10^6$	$9.4979 \cdot 10^{-3}$	$-1.7536 \cdot 10^3$
$2.0176 \cdot 10^{-3}$	$-7.1635 \cdot 10^5$	$10.709 \cdot 10^{-3}$	$4.0362 \cdot 10^2$
$3.3062 \cdot 10^{-3}$	$2.6774 \cdot 10^5$	$11.897 \cdot 10^{-3}$	$-6.5661 \cdot 10^1$
$4.5626 \cdot 10^{-3}$	$-1.1246 \cdot 10^5$	$13.010 \cdot 10^{-3}$	$5.5069 \cdot 10^0$
$5.8069 \cdot 10^{-3}$	$4.6500 \cdot 10^4$	$13.832 \cdot 10^{-3}$	$-5.6846 \cdot 10^{-1}$
$7.0440 \cdot 10^{-3}$	$-1.7827 \cdot 10^4$	$14.550 \cdot 10^{-3}$	$6.8010 \cdot 10^{-1}$
$8.2747 \cdot 10^{-3}$	$6.0685 \cdot 10^3$	$14.993 \cdot 10^{-3}$	$2.2835 \cdot 10^{-1}$

Table 3: The extrema of $\Lambda_{1000} \circ \cos$ and their abscissas in $[0, 0.014993]$

6. Conclusions

In the paper we have presented a method for fast and memory efficient evaluation within any precision of high degree spherical polynomials at many scattered points on the sphere. As shown in §4.3 the method can also be used for approximation on the sphere, verification of spherical polynomials, and for fast generation of surfaces in computer-aided geometric design.

Some of the distinctive features of our algorithm are:

- The evaluation is done by formula (2.30) which has two loosely connected parts: the nodes and cubatures weighs on the one hand and the kernel Λ_N and the radius of the point δ-neighborhood on the other hand. This relation allows a wide variety of nodal sets, polynomial degrees and precisions to be covered by one and the same formula.
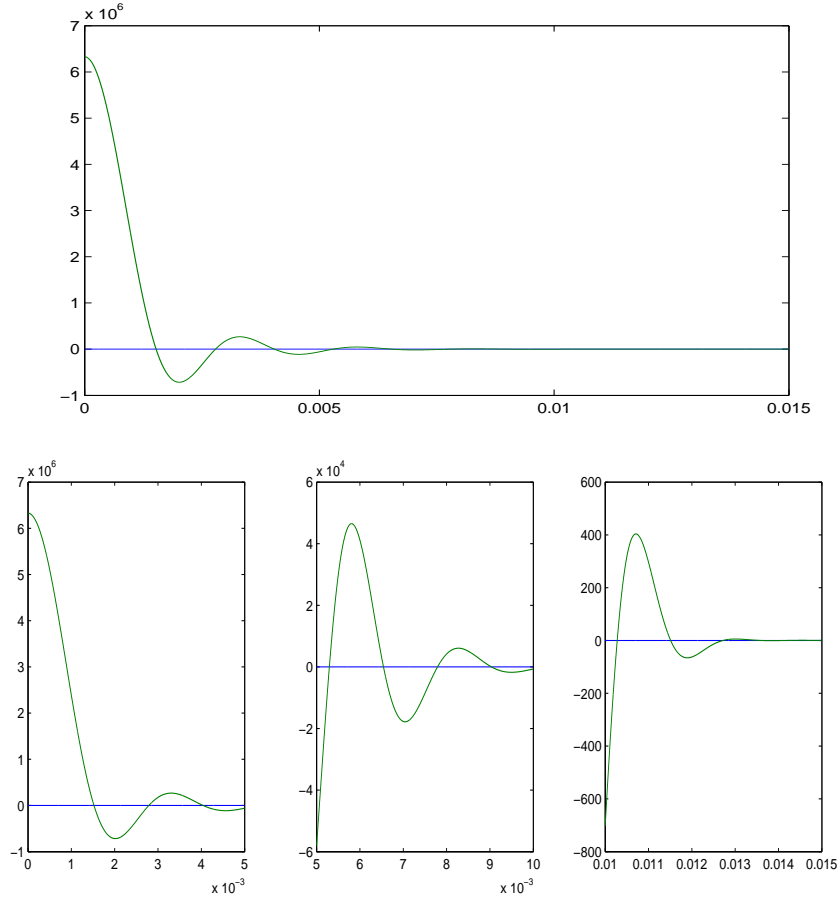
FIGURE 3. Graph of $\Lambda_{1000} \circ \cos$ in $[0, 0.014993]$

- The product $N\delta$ depends logarithmically on ε, which allows the algorithm to work with *practically the same speed* for widely varying precisions ε. At the same time the speed *does not depend on the polynomial degree.* Thus very high degrees and very fine precisions are attainable for effective computation.
- The algorithm error is measured in the *uniform norm*, which guarantees the computational accuracy at any point from the sphere. This feature gives our algorithm an important advantage over algorithms with error estimates in average, in RMS or of statistical nature.
- The *local* nature of formula (2.30) implies that only nodes which are close to the point of interest enter the computations, even if the polynomial is highly oscillating (see Example 1 in §5). As a consequence, when computations for a given region are performed only the grid values covering the region plus a small neighborhood have to be stored in the computer memory.
- The local nature of the method also leads to its *natural parallelization.*

- The improvement of the precision ε is achieved by increasing δ and does not require polynomial values at new nodal points. Such increase of δ increases the complexity, thus an application of the algorithm in a nested fashion may be used for gaining speed (see §3.7).
- One of the main ways for increasing the speed of the algorithm is the increasing of the parameter α as (3.43) shows. Under certain conditions α can be chosen larger than the main restriction from (2.34) allows (see §4.2 and Example 2 of §5).
- The kernels Λ_N are *"universal"* in the following senses: (a) One can apply (2.30) with many different nodal sets (and cubatures) with the same kernel; (b) One can achieve precision ε varying in a logarithmically wide range with the same kernel.
- The algorithm can work with, but does nor require, asymptotically equally spaced nodes, such as HEALPix or GLESP. The use of regular nodal sets, as those from §2.2, facilitates the easy determination of the nodes from a point δ-neighborhood.
- For a given nodal set $\mathcal{X}$ one can use different cubatures satisfying the common requirement of high degree of exactness.
- The method is *numerically stable* due to the small number of operations needed to compute the values of the approximant given in (2.30).
- The method successfully *avoids underflow and overflow* problems since no evaluation of a single associated Legendre function is performed. We only use downward Clenshaw summation with the Legendre polynomials recurrence.
- The advantage of our algorithm over the direct calculation of spherical polynomials becomes significant for spherical polynomials of degrees higher than 300.

REFERENCES

[1] C. W. Clenshaw, A. R. Curtis, A method for numerical integration on an automatic computer, Numer. Math. **2** (1960) 197-205.
[2] J. R. Driscoll, D. M. Healy, Computing Fourier Transforms and Convolutions on the 2-Sphere, Adv. in Appl. Math. **15** (1994), 202-250.
[3] A. Erdélyi, W. Magnus, F. Oberhettinger and F. G. Tricomi, *Higher Transcendental Functions*, Vol. **2**, McGraw-Hill, New York, 1953.
[4] Leopold Fejér, On the infinite sequences arising in the theories of harmonic analysis, of interpolation, and of mechanical quadratures, Bull. Amer. Math. Soc. **39** (1933), 521534.
[5] Leopold Fejér, Mechanische Quadraturen mit positiven Cotesschen Zahlen, Math. Z. **37** (1933), 287-309.
[6] K. G. Ivanov, P. Petrushev, Yuan Xu, Sub-exponentially localized kernels and frames induced by orthogonal expansions, Math. Z. DOI 10.1007/s00209-008-0469-4, 2009 (to appear).
[7] K. G. Ivanov, P. Petrushev, Yuan Xu, Decomposition of spaces of distributions induced by tensor product bases, Math. Nachr. (to appear).
[8] M.-J. Lai, L. Schumaker, *Spline Functions on Triangulations*, Cambridge University Press, 2007.
[9] M. Mohlenkamp, A Fast Transform for Spherical Harmonics, J. Fourier Anal. Appl. **5** (1999), 159-184.
[10] H. Moritz, B. Hofmann-Wellenhof, *Physical Geodesy*, Springer Wein New York Publishing, 2006.
[11] F. J. Narcowich, P. Petrushev and J. D. Ward, Localized tight frames on spheres, SIAM J. Math. Anal. **38** (2006), 574-594.

[12] F. J. Narcowich, P. Petrushev and J. D. Ward, Decomposition of Besov and Triebel-Lizorkin spaces on the sphere, J. Funct. Anal. **238** (2006), 530-564.

[13] P. Nevai, Orthogonal Polynomials, Memoirs of AMS, Vol. **18**, 1979.

[14] N.K. Pavlis, S.A. Holmes, S.C. Kenyon, and J.K. Factor, An Earth Gravitational Model to Degree 2160: EGM2008, presented at the 2008 General Assembly of the European Geosciences Union, Vienna, Austria, April 13-18, 2008.

[15] E. Stein, G. Weiss, *Fourier analysis on Euclidean spaces*, Princeton University Press, Princeton, New Jessey, 1971.

[16] M. Tygert, Fast algorithms for spherical harmonic expansions II, J. Comput. Phys. **227** (2008), 4260-4279.

[17] G. Szegő, *Orthogonal Polynomials*, Amer. Math. Soc. Colloq. Publ. Vol. **23**, Providence, 4th edition, 1975.

Institute of Mathematics and Informatics, Bulgarian Academy of Sciences, 1113 Sofia, Bulgaria

E-mail address: kamen@math.bas.bg

Department of Mathematics, University of South Carolina, Columbia, SC 29208, and Institute of Mathematics and Informatics, Bulgarian Academy of Sciences

E-mail address: pencho@math.sc.edu